

Co-Editor Decision: Publish subject to minor revisions (review by editor) (14 Dec 2017)
by Rob MacKenzie

Comments to the Author:

Dear Dr Evangeliou and colleagues,

Thank you for your patience; we have struggled to find referees with time to provide a review, but I am glad that we have in the end got two informative reviews. I am pleased to accept your paper for ACP subject to the revisions outlined below, which derive from reviewers comments that I don't think you have quite fully satisfied yet,

Sincerely,

Rob MacKenzie

Response: We appreciate Editor's efforts to get reviews as fast as possible. We have tried to satisfy the comments that Editor considers so important in order our article to be published in ACP.

Abstract and elsewhere: to avoid the potential for misunderstandings, I suggest reporting the modulus of the FB accompanied by the word 'underestimate'. You should report the RMSE results as well as FB in the abstract.

Response: Corrected! See manuscript with track changes in abstract and elsewhere.

Lines 50-52: I don't think you can use the terms "quite accurately" and "small discrepancies" when you have already reported $|FB| > 100\%$ a few lines above. Please find a more specific summary of the model evaluation.

Response: Corrected! See line 52.

Lines 52-54. I don't see how this final sentence follows from what went before. I suggest you state that your independent datasets were 50% lower than your own measurements at line 50.

Response: We agree that this sentence does not follow what is stated above and we have removed it. Paragraph now ends with line 53.

Line 80 ppb here is presumably mass/mass (ng/g). Better to be explicit, I think, so as not to hold up the reader.

Response: Corrected! Please see line 88.

In the discussion on lines 120-124, and in Figure 1, please refer the reader to Table S1.

Response: Corrected! Please see paragraph in lines 129-141.

For Figure 1c, please refer to Silverstein et al. (2008) and try to find a better colour map.

Response: Corrected! Though, we do not understand how a publication entitled “Automatic Perceptual Color Map Generation for Realistic Volume Visualization” is related with a plot that uses default colorbars from the matplotlib library of the open access Python language.

We have included the reference in the manuscript (line 879) and we have tried to use another colorbar for Fig. 1(c) (see line 873).

Line 180. Do you really mean that trajectories were released at 20km altitude? This is well inside the polar stratosphere and so very unlikely to contribute to wet deposition at the trajectory endpoints.

Response: The right statement is that the computational particles were released between 0 and 20,000 meters.

We know that 20 km is a stratospheric altitude. However, from tests that we have made, we have found that this is the optimal altitude in order to account for all wet scavenging processes that occur in the atmosphere. I admit that if we release the same computational particles within 0-8,000 meters or less, we may end up with the same results. It does not cost anything to us (except for some additional computational time) to account for higher altitudes though. Please see all the tests made in <https://www.geosci-model-dev.net/10/4605/2017/>.

Line 217 or thereabouts. Please insert a short subsection prefacing your approach to the statistics you will use to report measurements and the statistics you will use to compare model and measurements. You can move the material around line 260 to here to consolidate. This way you will set out your approach ahead of reporting the results. Readers may not agree completely with your approach, but at least they will know what it is and get used to it. In the current version, queries about the statistical approach get in the way of considering the scientific implications of the actual results. I would encourage you to draw the reader’s attention to figures such as S1 and S3 in this discussion, because these show clearly that summary statistics of central tendency and RMSE need to be interpreted with care. Figure S3 particularly shows the well-known property of the correlation coefficient that it can report a high value (goodness of fit) for an observation vs model scattergram with gradient very different from unity.

Response: Corrected! We have added a paragraph after section 3 about the statistical tools that we have used. We have highlighted Figures S1 – S3 as the figures that summarize our findings (lines 232-245).

Line 223 and elsewhere. Please don’t mix resistant and robust statistical measures (percentiles) with non-resistant and non-robust measures (range, mean, and standard deviation). Report mean together with standard deviation, and median together with quartiles. It is perfectly possible to estimate percentiles for a sample of 10 or 11 – see a standard statistics textbook, or <http://www.itl.nist.gov/div898/handbook/prc/section2/prc262.htm> for a quick hint.

Response: We agree with this comment and we have corrected the manuscript wherever needed. Please see track changes in the manuscript.

Lines 268-270. The discussion of FB gets very convoluted here, with positive and negative numbers in close proximity. I realise it's awkward, but please look at simplifying, perhaps by talking about the modulus of FB.

Response: Corrected! We have tried to do this wherever it was possible and we have also reformulated many sentences in this direction. Please see track changes in the manuscript.

Lines 296-300. Please report medians and percentiles from the literature, rather than just upper limits.

Response: In this section, we report concentrations from the literature as the reviewer has pointed out. Although we have all the data presented in Doherty et al. or MacDonald et al. papers and we could perform any kind of statistics, we have not all the observations from Aamaas et al. (2011), Ruppel et al. (2014), McConnel et al. (2007), Forsstrom et al. (2013) or Svensson et al. (2013). Since we report values as ranges (Min–Max concentrations) for all the aforementioned studies, we think that it would be awkward to report median +/- quartiles for Deherty et al. (2010) and MacDonald et al. (2017). For better consistency in the current paragraph, we would like to keep ranges for all the measurements collected from the relevant literature. We hope that the Editor will understand and agree.

Line 392. Remove double full stop.

Response: Corrected (line 473).

Line 402. Representing the Doherty et al. (2010) data as a mean with standard deviation leads you to reporting a standard deviation bigger than the mean. For data that is positive definite this simply illustrates the difficulties of working with assumed Gaussian statistics on highly skew data. I suggest you replace with median and interquartile range.

Response: This problem of reporting higher standard deviations than the mean can also occur when presenting median and interquartile ranges (see, for instance, corrected values for our campaign in 2014). We have substituted mean+/-sd with median+/- interquartile ranges! See lines 485-487, and 493-494.

Lines 414-415. I would suggest replacing “no safe conclusions” with a statement that it is not clear whether the discrepancy arises as a measurement artefact (even though every effort has been taken in both papers to follow a robust protocol) or from real spatio-temporal variation.

Response: Corrected. See lines 498-500.

Reference

Silverstein, J., Parsad, N., and Tsirlina, V. (2008). Automatic perceptual color map generation for realistic volume visualization. *Journal of Biomedical Informatics*, 41(6):927.

1 **Origin of elemental carbon in snow from Western Siberia**
2 **and northwestern European Russia during winter–spring**
3 **2014, 2015 and 2016**

4

5 **Nikolaos Evangeliou^{1,*}, Vladimir P. Shevchenko², Karl Espen Yttri¹, Sabine**
6 **Eckhardt¹, Espen Sollum¹, Oleg S. Pokrovsky^{3,4}, Vasily O. Kobelev⁵, Vladimir B.**
7 **Korobov⁶, Andrey A. Lobanov⁵, Dina P. Starodymova², Sergey N. Vorobiev⁷,**
8 **Rona L. Thompson¹, Andreas Stohl¹**

9

10 ¹ NILU - Norwegian Institute for Air Research, Department of Atmospheric and Climate
11 Research (ATMOS), Kjeller, Norway.

12 ² Shirshov Institute of Oceanology, Russian Academy of Sciences, Nakhimovsky prospect 36,
13 117997 Moscow, Russia.

14 ³ Geosciences Environment Toulouse, UMR 5563 CNRS, University of Toulouse, 14 Avenue
15 Edouard Belin, 31400, Toulouse, France.

16 ⁴ N. Laverov Federal Center for Integrated Arctic Research, Russian Academy of Science,
17 Sadovaya street, 3, 163000, Arkhangelsk, Russia.

18 ⁵ Arctic Research Center of the Yamalo-Nenets autonomous district, Vos'moy proezd, NZIA
19 building, 629730, Nadym, Yamalo-Nenets autonomous district, Russia.

20 ⁶ North-Western Branch of Shirshov Institute of Oceanology, Russian Academy of Sciences,
21 Naberezhnaya Severnoy Dviny 112/3, 163061, Arkhangelsk, Russia.

22 ⁷ BIO-GEO-CLIM Laboratory, Tomsk State University, 36 Prospect Lenina, 634050, Tomsk,
23 Russia.

24

25 *Correspondence to: N. Evangeliou, NILU - Norwegian Institute for Air Research,
26 Department of Atmospheric and Climate Research (ATMOS), Kjeller, Norway
27 (Nikolaos.Evangeliou@nilu.no)

28

29 **Abstract**

30 Short-lived climate forcers have been proven important both for the climate and human
31 health. In particular, black carbon (BC) is an important climate forcer both as an aerosol and
32 when deposited on snow and ice surface, because of its strong light absorption. This paper
33 presents measurements of elemental carbon (EC; a measurement-based definition of BC) in
34 snow collected from Western Siberia and northwestern European Russia during 2014, 2015
35 and 2016. The Russian Arctic is of great interest to the scientific community due to the large
36 uncertainty of emission sources there. We have determined the major contributing sources of
37 BC in snow in Western Siberia and northwestern European Russia using a Lagrangian
38 atmospheric transport model. For the first time, we use a recently developed feature that
39 calculates deposition in backward (so-called retroplume) simulations allowing estimation of
40 the specific locations of sources that contribute to the deposited mass.

41 EC concentrations in snow from Western Siberia and northwestern European Russia
42 were highly variable depending on the sampling location. Modelled BC and measured EC
43 were moderately correlated ($R = 0.53 - 0.83$) and a systematic region-specific model
44 underestimation was found. Modelled underestimated observations by 42% (RMSE = 49 ng g⁻¹) in 2014, 48% (RMSE = 37 ng g⁻¹) in 2015 and 27% (RMSE = 43 ng g⁻¹) in 2016. For EC
45 sampled in northwestern European Russia the underestimation by the model was smaller
46 (fractional bias, FB > -100%). In this region, the major sources were transportation activities
47 and domestic combustion in Finland. When sampling shifted to Western Siberia, the model
48 underestimation was more significant (FB < -100%). There, the sources included emissions
49 from gas flaring as a major contributor to snow BC. The accuracy of the model calculations
50 was also evaluated using two independent datasets of BC measurements in snow covering the
51 entire Arctic. The model underestimated BC concentrations in snow especially for samples
52 collected in springtime.

Nikolaos Evangeliou 18/12/2017 11:59
Formatted: Superscript

Nikolaos Evangeliou 18/12/2017 12:41
Deleted: reproduced

Nikolaos Evangeliou 18/12/2017 12:41
Deleted: snow

Nikolaos Evangeliou 18/12/2017 12:41
Deleted: quite accurately, although small discrepancies occurred

Nikolaos Evangeliou 18/12/2017 12:41
Deleted: mainly

Nikolaos Evangeliou 18/12/2017 12:44
Deleted: Nevertheless, EC concentrations in snow presented here are about 20% lower than previously reported ones in Western Siberia and northwestern European Russia.

64 1 Introduction

65 Black carbon (BC) is the strongest light-absorbing component of atmospheric aerosol
66 and is formed by the incomplete combustion of fossil fuels, biofuels, and biomass (Bond et
67 al., 2013). It is emitted directly into the atmosphere in the form of fine particles. BC is a major
68 component of “soot”, a complex light-absorbing mixture that also contains organic carbon
69 (OC) (Bond et al., 2004). Combustion sources emitting BC include open biomass burning
70 (forest, savanna, agricultural burning), residential biofuel combustion, diesel engines for
71 transportation or industrial use, industrial processes and power generation, or residential coal
72 combustion (Liu et al., 2011; Wang et al., 2011).

73 BC is important on a global perspective because of its impacts on human health and on
74 climate. As a component of fine particulate matter (PM_{2.5}), it is associated with negative
75 health impacts, including premature mortality (Lelieveld et al., 2015; Turner et al., 2005). It
76 absorbs solar radiation, has a significant impact on cloud formation and, when deposited on
77 ice and snow, it accelerates ice melting (Hansen and Nazarenko, 2004). BC has a lifetime that
78 can be as long as 9–16 days (Bond et al., 2013). After its emission, BC can travel over long
79 distances (Forster et al., 2001; Stohl et al., 2006) and reach remote areas such as the Arctic.
80 Arctic land areas are covered by snow in winter and spring, while the Arctic Ocean is partly
81 covered by ice. Sea ice has a much higher albedo (≈ 0.5 – 0.7) compared to the surrounding
82 ocean (≈ 0.06), thus presence of sea ice reduces the heat uptake of the ocean. Snow has an
83 even higher albedo than sea ice and can reflect as much as 90% of the incoming solar
84 radiation (Brandt et al., 2005; Singh and Haritashya, 2011). BC deposited on ice lowers its
85 albedo, increases heat uptake by sea ice, accelerates its melting, and therefore decreases
86 surface albedo both directly and indirectly.

87 Hegg et al. (2009) reported that snow in the Arctic often contains BC at concentrations
88 between 1 and 30 $\mu\text{g g}^{-1}$, which can cause a snow albedo reduction of 1–3% in fresh snow and
89 another 3–9% as snow ages and BC becomes more concentrated near the surface (Clarke and
90 Noone, 1985). This solar radiation reflecting capacity of snow insulates the sea ice, maintains
91 cold temperatures and delays ice melt in summertime. After the snow begins to melt and
92 because shallow melt ponds have an albedo of approximately 0.2 to 0.4, the surface albedo
93 drops to about 0.75 or even lower (0.15) as melt ponds grow and deepen (Singh and
94 Haritashya, 2011). These changes have been found to be important for the global energy

Nikolaos Evangeliou 18/12/2017 12:49

Deleted: ppb

Nikolaos Evangeliou 18/12/2017 12:49

Formatted: Superscript

96 balance (Flanner et al., 2007; Hansen and Nazarenko, 2004) and, if enhanced by BC,
97 contribute to climate warming (Warren and Wiscombe, 1980).

98 Although BC in Arctic snow and ice has been found to be important for the Earth's
99 climate (Flanner et al., 2007; Sand et al., 2015), its large-scale temporal and spatial
100 distributions and exact origin are still poorly quantified (AMAP, 2015). Efforts to determine
101 the concentrations of BC in snow across the Arctic were made by Clarke and Noone (1985),
102 Doherty et al. (2010, 2013), Forsström et al. (2013), Ingvander et al. (2013) and McConnell et
103 al. (2007). This paper presents measurements of Elemental Carbon (EC) concentrations in
104 snow samples collected in spring 2014, 2015 and 2016 in the Kindo Peninsula (White Sea,
105 Karelia), around Arkhangelsk in northwestern European Russia, and in Western Siberia. In
106 the latter area, gas flaring emissions are very important. Flaring emissions are highly
107 uncertain because both activity data and emission factors are largely lacking. According to the
108 Global Gas Flaring Reduction Partnership (GGFR)
109 (<http://www.worldbank.org/en/programs/gasflaringreduction>), nearly 50 billion m³ of gas are
110 flared in Russia annually. The Russian flaring emissions in the Nenets/Komi regions and in
111 Khanty-Mansiysk are the major sources in Western Siberia and northwestern European
112 Russia. It has been reported that gas flaring in Russia contributes about 42% to the annual
113 average BC surface concentrations in the Arctic (Stohl et al., 2013).

114 The use of the terms EC and BC has been the topic of several scientific papers (for
115 example, Andreae and Gelencsér, 2006; Bond et al., 2013; Petzold et al., 2013). Petzold et al.
116 (2013) defined BC as a substance with 5 properties (see Table 1 in Petzold et al., 2013), for
117 which no single measurement instrument exists that is sensitive to all of them at the same
118 time. Consequently, BC cannot uniquely be measured, although some of its properties can,
119 such as the absorption coefficient σ_{ap} and the elemental carbon (EC) concentration, both
120 commonly measured in atmospheric monitoring networks across the world. Hence, the term
121 BC should be used qualitatively.

122 In the present study, EC concentrations on ice from three campaigns measured with
123 Thermal–Optical Analysis (TOA) (see section 2.2) are compared to simulation results from
124 the Lagrangian particle dispersion model (LPDM) FLEXPART. The model is used here for
125 the first time to quantify the sources contributing to BC in snow in Russia adopting a special
126 feature that was developed recently.

127 2 Methodology

128 2.1 Collection and storage of snow samples

129 Fresh snow samples were collected along a north–south transect between Tomsk and
130 the Yamal coast in February–March 2014 (23 samples, [Table S 1](#)), while in March 2015
131 sample collection took place in the Kindo Peninsula and near the port of Arkhangelsk in the
132 White Sea (11 samples, [Table S 1](#)). Finally, in February–May 2016 samples were collected in
133 the Kindo Peninsula, in Arkhangelsk and between Tomsk and Yamal (20 samples, [Table S 1](#)).
134 These areas have been reported to receive pollution both from urban and gas flaring sources
135 (Stohl et al., 2013). For example, the gas flaring sources located in Yamal and Khanty-
136 Mansiysk (Russia) are in the main pathway along which sub-Arctic air masses travel to the
137 Arctic (Stohl et al., 2006). All sampling points were located more than 500 m away from
138 roads to minimize the direct influence from local traffic emissions. Information about sample
139 collection such as the location of sampling, the amount of snow collected and the depth at
140 which snow was sampled is reported in [Table S 1](#), and the sample locations are plotted in
141 [Figure 1](#).

142 Sampling was performed using a metal-free technique using pre-cleaned plastic shovels
143 and single-use vinyl gloves. Samples were stored in polyethylene bags which had been
144 thoroughly washed with 1 M HCl and rinsed with abundant deionised ultrapure water in the
145 laboratory prior to their use. After returning the samples to the laboratory, the snow was
146 allowed to melt at ambient temperature (18–20°C), and immediately filtered through quartz
147 47 mm fibre filters (2500QAT-UP Pall for samples collected in 2014 and QM-A Whatman for
148 samples collected in 2015 and 2016). The filters were dried at 60–70°C, wrapped in
149 aluminum foil and stored in a refrigerator. Quartz fiber filter collection efficiency of BC in
150 liquid samples can be less than 100% (Hadley et al., 2010; Ogren et al., 1983). To what extent
151 this has affected the levels reported in the present study is unknown. Thus the results
152 presented should be regarded as conservative estimates based on the assumption that some
153 BC might have been lost during filtration.

154 2.2 Elemental Carbon measurements by Thermal–Optical Analysis (TOA)

155 Elemental carbon (EC) content of the filters was measured at NILU’s laboratories by thermal-
156 optical analysis (TOA), using the Sunset laboratory OC/EC instrument operated according to
157 the EUSAAR-2 protocol (Cavalli et al., 2010). A 1.5 cm² punch was cut from the filtered
158 snow samples for the analysis. Transmission was used for organic carbon (OC) charring

Nikolaos Evangeliou 18/12/2017 12:56

Deleted:

Nikolaos Evangeliou 18/12/2017 12:56

Deleted: Figure 1

Nikolaos Evangeliou 18/12/2017 12:56

Deleted: Table S1

Nikolaos Evangeliou 18/12/2017 17:15

Deleted: Figure 1

163 correction. Performance of the OC/EC instrument's is regularly intercompared as part of the
164 joint European Monitoring and Evaluation Programme (EMEP) Aerosols, Clouds, and Trace
165 gases Research InfraStructure Network (ACTRIS) quality assurance and quality control effort
166 (Cavalli et al., 2015).

167 **2.3 Measurements of carbonate (CO_3^{2-})-carbon by Thermal-Optical Analysis** 168 **(TOA) following thermal-oxidative pre-treatment**

169 The content of carbonate (CO_3^{2-})-carbon on the filters was measured by TOA,
170 following thermal-oxidative pretreatment based on the approach described by Jankowski et al.
171 (2008). A punch of 1.5 cm² from each filter was heated at 450 °C for 2 hours in ambient air to
172 remove OC and EC, but not CO_3^{2-} -carbon. The filter punch was subjected to TOA
173 immediately (30 sec) after thermal-oxidative pre-treatment. The split time (between OC and
174 EC) obtained for each filter punch used to determine the filter samples' content of EC (section
175 2.2) was also used to apportion CO_3^{2-} -carbon to OC and/or EC. The influence of CO_3^{2-} -
176 carbon evolving as EC, was accounted for by the following equation:

$$EC_{CO_3^{2-}}^{corr} = EC - EC_{CO_3^{2-}}$$

177 where $EC_{CO_3^{2-}}^{corr}$ is elemental carbon corrected for CO_3^{2-} -carbon that evolved as EC during
178 TOA, EC is elemental carbon and $EC_{CO_3^{2-}}$ is CO_3^{2-} -carbon that evolved as EC during TOA.
179 Applying this correction, EC values were 5-22% lower (see Supplementary Information).

180 **2.4 Emissions and modelling of black carbon**

181 The concentrations of BC in snow were simulated with the LPDM FLEXPART version
182 10 (Stohl et al., 1998, 2005). The model was driven with operational meteorological wind
183 fields retrieved from the European Centre for Medium-Range Weather Forecasts (ECMWF)
184 of 3-hour (for the years 2014 and 2015) and hour (for the year 2016) temporal resolution. The
185 ECMWF data have 137 vertical levels and a horizontal resolution of 1°×1° for the 2014 and
186 2015 simulations and 0.5°×0.5° for the 2016.

187 The simulations were conducted in backwards time ("retroplume") mode, using a new
188 feature of FLEXPART to reconstruct wet and dry deposition with backward simulations
189 (Eckhardt et al., 2017). This new feature is an extension of the traditional possibility to
190 simulate atmospheric concentrations backward in time (Seibert and Frank, 2004; Stohl et al.,
191 2003). It is computationally efficient because it requires only two single tracer transport

192 simulations (one for wet deposition, one for dry deposition) for each measurement sample. To
193 reconstruct wet deposition amounts of BC, computational particles were released at altitudes
194 of 0 to 20 km at the locations where snow samples were taken, whereas to reconstruct dry
195 deposition, particles were released between the surface and 30 m at these locations. All
196 released particles represent a unity deposition amount, which was converted immediately (i.e.,
197 upon release of a particle) to atmospheric concentrations using the deposition intensity as
198 characterized either by dry deposition velocity or scavenging rate (for further details, see
199 Eckhardt et al., 2017). The concentrations were subsequently treated as in normal
200 “concentration mode” backward tracking (Seibert and Frank, 2004) to establish source-
201 receptor relationships between the emissions and deposition amounts. The termination time of
202 the particle release was the time at which the snow sample was collected, whereas the
203 beginning time was set as the time when the ECMWF precipitation at the sampling site,
204 accumulated backward in time, was equal to the water equivalent of the snow sample, up to
205 the specified sampling depth.

206 The model output consists of a spatially gridded sensitivity of the BC deposition at the
207 sampling location (receptor) to the BC emissions, equivalent to the backwards time mode
208 output for concentrations (Seibert and Frank, 2004; Stohl et al., 2003). BC deposition at the
209 snow sampling point can be computed (in mass per unit area) by multiplying the emission
210 sensitivity in the lowest model layer (the footprint emission sensitivity) with gridded
211 emissions from a BC emission inventory and integrating over the grid. The deposited BC can
212 be easily converted to BC snow concentration by taking into account the water equivalent
213 depth of the snow from ECMWF (in mm). In the present study, the ECLIPSE (Evaluating the
214 CLimate and Air Quality ImPacts of ShortlivEd Pollutants) version 5 emission inventory
215 (Klimont et al., 2016; Stohl et al., 2015) was used
216 (http://www.iiasa.ac.at/web/home/research/researchPrograms/air/Global_emissions.html).

217 The total emissions of BC from ECLIPSE in the areas of study are shown in [Figure 1](#), (left
218 panel).

219 BC was assumed to have a density of 2 g m^{-3} in our simulations and a logarithmic size
220 distribution with an aerodynamic mean diameter of $0.25 \text{ }\mu\text{m}$ and a logarithmic standard
221 deviation of 0.3. Each computational particle released in FLEXPART represents an aerosol
222 population with a lognormal size distribution (see Stohl et al., 2005). Assumed aerodynamic
223 mean diameter and logarithmic standard deviation are used by FLEXPART’s dry deposition
224 scheme, which is based on the resistance analogy (Slinn 1982), and they are consistent with

Nikolaos Evangeliou 18/12/2017 17:15
Deleted: Figure 1

226 those used in other transport models (see Evangeliou et al., 2016; Shiraiwa et al., 2008).
227 Below-cloud scavenging was determined based on the precipitation rate taken from ECMWF.
228 The in-cloud scavenging was based on cloud liquid water and ice content, precipitation rate
229 and cloud depth from ECMWF (Grythe et al., 2017). The FLEXPART user manual (available
230 from <http://www.flexpart.eu>) provides more information. All modelling results for this
231 sampling campaign can be viewed interactively at the URL
232 http://niflheim.nilu.no/NikolaosPY/SnowBC_141516.py.

233 3 Results

234 In this section the main results of EC concentrations in snow are presented, in contrast
235 to simulated BC concentrations with FLEXPART. The statistical dependence of the datasets
236 is assessed using the Pearson product-moment correlation coefficient. For further validation,
237 the fractional bias (FB) of each individual sample was calculated together with the mean
238 fractional bias (MFB) for observed and modelled concentrations as follows:

$$FB = \frac{C_m - C_o}{(C_m + C_o)/2} \times 100\% \text{ and } MFB = \frac{1}{N} \sum_{i=1}^N \frac{C_m - C_o}{(C_m + C_o)/2} \times 100\%$$

239 where C_m and C_o are the modelled BC and measured EC concentrations and N is the total
240 number of observations for each year. FB is a useful model performance indicator because it
241 is symmetric and gives equal weight to underestimations and overestimations (it takes values
242 between -200% and 200%). It is used here to show the locations where modelled BC
243 concentrations in snow over- or underestimate observations. Finally, for the same reasons, the
244 root mean square error (RMSE) was also computed, which is frequently used to measure
245 differences between values predicted by a model and the values actually observed (see Figure
246 S 1– S 3).

247 3.1 Elemental Carbon concentrations measured in snow

248 The spatial distribution of EC measured in snow samples from northwestern European
249 Russia and Western Siberia is shown in [Figure 1\(c\)](#) for each of the campaigns (2014, 2015
250 and 2016) and are also summarised in [Table S 2](#). There was large spatial variability in the
251 distribution of EC in snow in 2014 ranging from 3 to 219 ng g⁻¹, with a median (±interquartile
252 range) of 23±49 ng g⁻¹. The highest EC concentrations in 2014 were observed in Western
253 Siberia near Tomsk (147 to 219 ng g⁻¹). FLEXPART emission sensitivities for these samples

Nikolaos Evangeliou 18/12/2017 15:26
Moved (insertion) [1]

Nikolaos Evangeliou 18/12/2017 15:27
Deleted: EC

Nikolaos Evangeliou 18/12/2017 15:27
Deleted: BC

Nikolaos Evangeliou 18/12/2017 15:27
Deleted: for the 2014, 2015 and 2016 sampling campaigns

Nikolaos Evangeliou 18/12/2017 15:28
Moved (insertion) [2]

Nikolaos Evangeliou 18/12/2017 17:15
Deleted: Figure S 1

Nikolaos Evangeliou 18/12/2017 17:15
Deleted: Figure 1

Nikolaos Evangeliou 18/12/2017 15:37
Deleted: standard deviation

Nikolaos Evangeliou 18/12/2017 15:38
Deleted: 50

262 showed that the air was coming from the north and the east (see in
263 http://niflheim.nilu.no/NikolaosPY/SnowBC_141516.py). This explains the high
264 concentrations of EC, as most of the anthropogenic BC sources are located in these regions.
265 In the rest of the snow samples for 2014, EC concentrations between 4 and 170 ng g⁻¹ were
266 observed. High concentrations were observed near the Ob River coinciding with air masses
267 arriving mainly from Europe. During the 2015 field campaign, EC concentrations were the
268 highest near Arkhangelsk (175 ng g⁻¹), for which FLEXPART showed that the air was coming
269 from nearby areas (http://niflheim.nilu.no/NikolaosPY/SnowBC_141516.py). Therefore, it is
270 likely that the samples were affected by direct emissions from the city or the port of
271 Arkhangelsk. During the same campaign, snow samples collected in the Kindo peninsula (on
272 the White Sea coast) showed high variability in EC concentrations (range: 46 – 152 ng g⁻¹,
273 median=70±34 ng g⁻¹). According to FLEXPART emission sensitivities, air masses were
274 transported to Kindo peninsula from central and southern Europe driven by an anticyclone
275 over Scandinavia (http://niflheim.nilu.no/NikolaosPY/SnowBC_141516.py). Finally, for the
276 snow samples collected outside Arkhangelsk, at the Kindo peninsula, and close to the Yamal
277 Peninsula in Western Siberia in 2016, EC concentrations ranged between 7–161 ng g⁻¹
278 (median: 40±47 ng g⁻¹). Outside Arkhangelsk, EC concentrations varied widely from 31 to
279 161 ng g⁻¹ with a median concentration in this region of 61±43 ng g⁻¹. This is far below the
280 175 ng g⁻¹ observed in 2015, although there was only one sample collected in that year. In the
281 Kindo Peninsula, EC was relatively constant in 2016 ranging between 25 and 35 ng g⁻¹
282 (median = 28±4 ng g⁻¹), which is more than 60% lower compared with the 2015 values
283 (median = 70±34 ng g⁻¹). Finally, between Tomsk and Yamal, EC concentration was highly
284 variable (7 – 119 ng g⁻¹) due to the different EC sources affecting snow (median = 50±34 ng
285 g⁻¹). For instance, it is expected that gas flaring affects snow close to Yamal, while snow
286 collected in the south (Tomsk) is likely influenced by sources in Europe or local urban
287 emissions. Nevertheless, the highest concentrations (>100 ng g⁻¹) were observed north of
288 68°N, in the Yamal Peninsula.

289 We compared the measured EC concentrations in the snow samples with those
290 calculated by FLEXPART. For this, the emission sensitivities were multiplied with the total
291 emission fluxes from ECLIPSE (section 2.4). A scatter plot of modelled and measured snow
292 concentrations is presented in [Figure 1](#), (b). The results show a good correlation between
293 modelled BC and measured EC concentrations for the 2015 and 2016 campaigns ($R_{2015} =$

Nikolaos Evangeliou 18/12/2017 15:39
Deleted: 37

Nikolaos Evangeliou 18/12/2017 15:39
Deleted: 39

Nikolaos Evangeliou 18/12/2017 15:40
Deleted: 45

Nikolaos Evangeliou 18/12/2017 15:39
Deleted: 37

Nikolaos Evangeliou 18/12/2017 15:40
Deleted: 38

Nikolaos Evangeliou 18/12/2017 17:15
Deleted: Figure 1

300 0.83 and $R_{2016} = 0.68$, p – value < 0.05), but weaker correlation for 2014 ($R_{2014} = 0.53$,
301 p – value < 0.05).

$$FB = \frac{C_m - C_o}{(C_m + C_o)/2} \times 100\% \text{ and } MFB = \frac{1}{N} \sum_{i=1}^N \frac{C_m - C_o}{(C_m + C_o)/2} \times 100\%$$

302 The FB for individual samples is shown in [Figure S 1](#). The MFB of the model for the
303 2014 snow measurements was -42% , which shows that the model underestimated
304 observations. In total, the model underestimated concentrations [by 30% – 168%](#) for 17 out of
305 23 samples, whereas for the rest (six samples) FB values ranged between 20% and 148%
306 (median [MFB: \$-56\% \pm 72\%\$](#)) ([Figure S 1](#)). In 2015, the model [underestimated observations by](#)
307 [48%](#) (median [MFB: \$-56\% \pm 29\%\$](#)) [for](#) 11 out of 12 [samples](#) (FB between -101% and -7% ,
308 [while one](#) value was found to be 12%). For 2016, FB values of the simulated concentrations
309 of BC in snow showed another set of underestimation (median: $-13\% \pm 60\%$) [between](#) 0.3%
310 [and 198%](#) for 12 out of 19 samples. For the remaining seven samples, the model predicted
311 higher concentrations compared with observations (10% to 75%) ([Figure S 1](#)). RMSE values
312 were estimated to be quite high, between 37 and 49 ng g^{-1} , due to the large variation of the
313 observed EC concentrations.

314 The levels of EC in snow presented here are relatively high compared to previously
315 reported concentrations in the Arctic. Apart from Aamaas et al. (2011) who measured
316 maximum EC concentration in snow close to the airport of Svalbard of more than 1000 ng g^{-1} ,
317 most of the reported levels of EC in the relevant literature are close to our findings. For
318 instance, Ruppel et al. (2014) found that EC concentrations have been increasing up to 103 ng
319 g^{-1} since 1970 in Svalbard. McConnell et al. (2007) reported that the BC concentrations
320 measured at the D4 ice-core site in Greenland were 10 ng g^{-1} , at maximum, which most likely
321 originated from biomass burning in the conifer-rich boreal forest of the Eastern and Northern
322 United States and Canada. Forsström et al. (2013) reported concentrations as high as 88 ng g^{-1}
323 in Scandinavia, and lower ones at higher latitudes (11–14 ng g^{-1} in Svalbard, 7–42 ng g^{-1} in
324 the Fram Strait, and 9 ng g^{-1} in Barrow). Svensson et al. (2013) collected snow samples from
325 Tyresta National Park and Pallas-Yllästunturi National Park in Sweden. Tyresta is a relatively
326 polluted site located circa 25 km from the city centre of Stockholm with a population of about
327 2 million people. Yllästunturi National Park is located in Arctic Finland and a clean site with
328 no major city influencing the local and regional air. The concentration of EC in Pallas-
329 Yllästunturi was between 0 and 140 ng g^{-1} , while in Tyresta the BC concentrations were up to

Nikolaos Evangeliou 18/12/2017 15:26

Moved up [1]: For further validation, the fractional bias (FB) of each individual sample was calculated together with the mean fractional bias (MFB) for observed EC and modelled BC for the 2014, 2015 and 2016 sampling campaigns as follows:

$$FB = \frac{C_m - C_o}{(C_m + C_o)/2} \times 100\% \text{ and } MFB = \frac{1}{N} \sum_{i=1}^N \frac{C_m - C_o}{(C_m + C_o)/2} \times 100\%$$

where C_m and C_o are the modelled BC and measured EC concentrations and N is the total number of observations for each year.

Nikolaos Evangeliou 18/12/2017 15:26

Formatted: Justified, Indent: First line: 1

Nikolaos Evangeliou 18/12/2017 15:28

Moved up [2]: FB is a useful model performance indicator because it is symmetric and gives equal weight to underestimations and overestimations (it takes values between -200% and 200%). It is used here to show the locations where modelled BC concentrations in snow over- or underestimate observations (see Figure S 1).

Nikolaos Evangeliou 18/12/2017 17:15

Deleted: Figure S 1

399 more than 7 times higher (53–810 ng g⁻¹). Furthermore, Doherty et al. (2010) in the most
400 complete dataset for the Arctic snow and ice BC reported highly variable concentrations (up
401 to 800 ng g⁻¹) for five consecutive years (2005–2009). Finally, in the most recent dataset for
402 snow BC, Macdonald et al. (2017) reported BC concentrations ranging from 0.3 to 15 ng g⁻¹
403 were reported for the samples collected near the Alert observatory (see section 4.1).

404 3.2 Sources and origin of BC

405 We further analysed the model output in order to calculate relevant contributions from
406 various BC source types to BC concentrations in snow (for method description, see section
407 2.4). ECLIPSE emissions include waste burning (WST), industrial combustion and processing
408 (IND), surface transportation (TRA), power plants, energy conversion, and extraction (ENE),
409 residential and commercial combustion (DOM), gas flaring (FLR), while biomass burning
410 (BB) emissions were adopted from the Global Fire Emissions Database, Version 4
411 (GFEDv4.1) (Giglio et al., 2013). The results are depicted in [Figure 2](#), for the sampling
412 campaigns of 2014, 2015 and 2016 in Western Siberia and North-Western European Russia,
413 sorted from the northernmost to the southernmost sampling location.

414 In 2014, TRA contributed about 18%, on average, to the simulated BC in snow, DOM
415 28%, FLR 44%, whereas ENE and IND were less significant. Maxima of TRA, DOM, and
416 FLR contributions were observed at a latitude of about 65°N, where measured EC and
417 modelled BC were similar. An example of the contribution from the aforementioned
418 dominant sources to snow BC concentrations for the highest measured EC concentration in
419 snow is shown in [Figure 3](#). The transport sector includes emissions from all land-based
420 transport of goods, animals and persons. It is more significant in southern Russia and close to
421 the borders with Kazakhstan and Mongolia, where a large number of major Russian cities
422 (e.g., Moscow, Kazan, Samara, Yekaterinburg, Tomsk, Novosibirsk, Krasnoyarsk, etc...) are
423 located and connected with each other by federal highways. Residential and commercial
424 combustion includes emissions from combustion in households and public and commercial
425 buildings. Therefore, it is expected to be high for areas that consist of large population centres
426 ([Figure 3](#)). FLR emissions were found to contribute the most in this example with a total
427 concentration from this sector of 19.7 ng g⁻¹ (compared with 12.6 and 16.5 ng g⁻¹ in TRA and
428 DOM, respectively) ([Figure 3](#)).

429 In the Kindo Peninsula and in Arkhangelsk, where snow sampling took place in 2015,
430 the main contributions to snow BC were from DOM (47%), TRA (30%), BB (7%), and FLR

Nikolaos Evangeliou 18/12/2017 17:15
Deleted: Figure 2

Nikolaos Evangeliou 18/12/2017 17:15
Deleted: Figure 3

Nikolaos Evangeliou 18/12/2017 17:15
Deleted: Figure 3

Nikolaos Evangeliou 18/12/2017 17:15
Deleted: Figure 3

435 | (6%) (see [Figure 2](#)). Similar to EC measurements in snow, simulated BC was also higher than
436 | in 2014, as the sampling sites were located closer to strong sources in Europe (Kindo) and
437 | close to a populated area (Arkhangelsk) with a strong regional impact. The highest
438 | concentration of EC was observed in the Kindo Peninsula (33.13°E – 66.53°N). [Figure 4](#)
439 | shows the spatial distribution of emissions that contributed to simulated snow BC at the
440 | sampling point where the highest BC concentration was observed. In this case, TRA and
441 | DOM emissions from Europe mostly affected snow in the Kindo Peninsula whereas FLR
442 | emissions were very low due to the long distance from the sampling point. Emissions from an
443 | unusual late winter/early spring episode of BB in the borders of Belarus, Ukraine and Russia
444 | also affected BC concentrations in snow in northwestern European Russia ([Figure 4](#)). The
445 | importance of episodic BB releases in Russia, the miscalculation of satellite retrieved BB
446 | emissions and their impact in Arctic concentrations in early spring has been explained by
447 | Evangeliou et al. (2016) and Hao et al. (2016). BB emissions, originating mostly from Eastern
448 | Europe, contributed about 19.4 ng g⁻¹ to the snow concentration at the receptor point ([Figure](#)
449 | [4](#)). TRA and DOM emissions were the dominant sources for this sampling point, contributing
450 | 33.6 and 47.2 ng g⁻¹, respectively ([Figure 4](#)).

451 | Finally, in 2016, when samples were collected at the Kindo Peninsula, in Arkhangelsk
452 | and in Yamal, DOM, FLR and TRA contributed, on average, 31%, 29% and 27%,
453 | respectively (see [Figure 2](#), (c)). Similar to the measured EC concentrations in snow, simulated
454 | concentrations of BC in 2016 were lower than those in 2015, on average. The highest
455 | measured EC concentration was observed in the Khanty-Mansiysk region (72.94°E –
456 | 65.36°N), which mirrors the simulated BC concentration at the same point very well. The
457 | much higher contribution from TRA at this sampling point (38.6 ng g⁻¹) ([Figure 5](#), (b)) is
458 | attributed to emissions from Southern Russia (e.g., Tomsk), where all the main cities in
459 | Russia are located. Another large fraction of TRA emissions comes from Central and Eastern
460 | Europe (see also in http://niflheim.nilu.no/NikolaosPY/SnowBC_141516.py). Similar to
461 | TRA, emissions from DOM were mostly transported to Khanty-Masiysk from Central and
462 | Eastern Europe, as well as from Turkey contributing 36.6 ng g⁻¹ ([Figure 5](#)). As previously
463 | mentioned, the sampling point where the highest EC concentration was measured is located
464 | inside the largest gas flaring region of Russia. In addition, the corresponding emission
465 | sensitivity maps showed that the air was coming from south passing directly through this high
466 | emission region making FLR emissions the highest contributing source (88.8 ng g⁻¹) ([Figure](#)
467 | [5](#)).

Nikolaos Evangeliou 18/12/2017 17:15
Deleted: Figure 2

Nikolaos Evangeliou 18/12/2017 17:15
Deleted: Figure 4

Nikolaos Evangeliou 18/12/2017 17:15
Deleted: Figure 4

Nikolaos Evangeliou 18/12/2017 17:15
Deleted: Figure 4

Nikolaos Evangeliou 18/12/2017 17:15
Deleted: Figure 4

Nikolaos Evangeliou 18/12/2017 17:15
Deleted: Figure 2

Nikolaos Evangeliou 18/12/2017 17:15
Deleted: Figure 5

Nikolaos Evangeliou 18/12/2017 17:15
Deleted: Figure 5

Nikolaos Evangeliou 18/12/2017 17:15
Deleted: Figure 5

477 4 Discussion

478 4.1 Cross validation of modelled BC concentrations with public datasets

479 In this section, we present an effort to further validate our model calculations of BC
480 concentrations in snow. For this purpose, BC concentrations in snow that were adopted from
481 Doherty et al. (2010) were compared with modelled BC concentrations in snow that were
482 simulated with FLEXPART as described in section 2.4. Samples were collected in Alaska,
483 Canada, Greenland, Svalbard, Norway, Russia, and the Arctic Ocean during 2005–2009, on
484 tundra, glaciers, ice caps, sea ice, frozen lakes, and in boreal forests. Snow was collected
485 mostly in spring, when the combination of snow cover and exposure to sunlight is at
486 maximum and before the snow had started to melt. Samples of melting snow collected in the
487 summer of 2008 from Greenland and from Tromsø, Norway, were removed from the study, as
488 we have no knowledge about the depth of the melt layer and effects of the percolation of
489 meltwater through the snowpack. All samples were collected away from local sources of
490 pollution. In many locations (Canadian Arctic, Russia, Greenland, Tromsø and Ny-Ålesund)
491 samples were gathered at different depths throughout the snowpack, giving information on the
492 seasonal evolution of BC concentrations as the snow accumulated (and/or sublimated)
493 throughout the winter. In these cases only the surface BC was taken into account. The snow
494 was melted and filtered, and the filters were analysed in a specially designed
495 spectrophotometer system to infer the concentration of BC (for more information see Doherty
496 et al., 2010). In contrast to our findings for the origin of snow BC in the Russian Arctic, a
497 source apportionment analysis performed in the 2008 and 2009 measurements (Hegg et al.,
498 2010) from this dataset showed that the dominant source of BC in the Arctic snow pack was
499 biomass burning. Specifically in Eastern Siberia biomass burning of crops and grasslands
500 contributed more snow BC in high latitudes than boreal forest fires, in contrast to the
501 Canadian Arctic.

502 A comparison of modelled (FLEXPART) and measured BC concentrations (Doherty et
503 al., 2010) in snow is depicted in [Figure S 2](#). The model captures snow BC concentrations
504 relatively well in most of the Arctic regions except for the Canadian Arctic, where the
505 modelled concentrations of snow in 2007 were significantly higher. Samples from the same
506 region in other years showed moderate agreement with modelled values. Similar to our
507 finding for the new Russian measurements, the model [underestimated deposition by 51%](#). The
508 RMSE was estimated to be 52 ng g⁻¹, which is acceptable considering that the variation of
509 snow concentrations in the dataset ranged from 0.3 to 783 ng g⁻¹. The highest measured

Nikolaos Evangeliou 18/12/2017 17:15

Deleted: Figure S 2

Nikolaos Evangeliou 18/12/2017 11:25

Deleted: output, with a MFB of -

Nikolaos Evangeliou 18/12/2017 11:26

Deleted: , tends to underestimate deposition.

513 concentrations of snow BC were observed in Russia, where the model showed a good spatial
514 agreement. For instance, the highest values were obtained in Western Siberia, close to the gas
515 flaring regions of the Nenets/Komi oblast, as well as in southeastern and northeastern Russia,
516 where air masses were arriving from high emitting sources in southeastern Asia. Lower biases
517 in modelled BC concentrations were observed in northern Siberia with the exception of a few
518 samples at the coasts of the Kara Sea and northeastern Siberia. Furthermore, biased BC
519 concentrations were also observed in Greenland and northern Canada. In Western Siberia, BC
520 in snow presented in Doherty et al. (2010) between 2005–2009 was 80 ± 63 ng g⁻¹ on average,
521 which is very close to the average value of measured EC obtained from the sampling 2014–
522 2016 campaigns (50 ± 46 ng g⁻¹).

523 From total number of samples presented in (Doherty et al., 2010) that were used here
524 for validation, only six were collected in the Yamal Peninsula similar as part of the data
525 presented in the current paper. The rest was collected in Nenets/Komi region and in Eastern
526 Russia and cannot be directly compared with snow EC measurements from the 2014 – 2016
527 campaigns. BC concentrations in Yamal Peninsula in 2007 ranged from 4.1 to 17.6 ng g⁻¹
528 (~~median±interquartile; 10.3±4.9~~ ng g⁻¹). In the same region, we report EC concentrations to be
529 more than double varying between 6.6 to 55 ng g⁻¹ (~~median±interquartile; 27.8±25.5~~ ng g⁻¹),
530 whereas there were two samples that showed EC concentrations of more than 100 ng g⁻¹. As
531 mentioned in section 2.1 the sampling of snow for the EC analysis took place more than 500
532 m away from roads to minimize influence from traffic emissions, while a similar statement is
533 also found in the Doherty et al. (2010) data. It is not clear whether the observed discrepancy
534 arises as a measurement artefact (even though every effort has been taken in both papers to
535 follow a robust protocol) or from real spatio-temporal variation.

536 Modelled BC concentrations simulated with FLEXPART were also compared with
537 snow BC concentrations from samples collected at the Global Atmosphere Watch
538 Observatory at Alert, Nunavut, from September 14th, 2014 to June 1st, 2015 and they are
539 available in Macdonald et al. (2016). Alert is a remote outpost in the Canadian high Arctic, at
540 the northern coast of Ellesmere Island (82°27' N, 62°30' W), with a small transient
541 population of research and military personnel. Sampling details and analytical methodologies
542 used for the analysis of BC can be found in Macdonald et al. (2016). BC concentrations in
543 FLEXPART were simulated as in all previous analyses described in this paper (see section
544 2.4.). Timeseries of simulated and measured BC are depicted in [Figure S 3](#), for the whole
545 sampling period. As before, a correlation coefficient (*R*) of 0.63 indicates that our model

Nikolaos Evangeliou 18/12/2017 16:50

Deleted: 10

Nikolaos Evangeliou 18/12/2017 16:50

Deleted: 13

Nikolaos Evangeliou 18/12/2017 16:49

Deleted: 83

Nikolaos Evangeliou 18/12/2017 16:49

Deleted: 37

Nikolaos Evangeliou 18/12/2017 16:58

Deleted: Average

Nikolaos Evangeliou 18/12/2017 17:00

Deleted: 5

Nikolaos Evangeliou 18/12/2017 16:58

Deleted: D

Nikolaos Evangeliou 18/12/2017 16:58

Deleted: 1

Nikolaos Evangeliou 18/12/2017 16:58

Deleted: 8

Nikolaos Evangeliou 18/12/2017 17:00

Deleted: Average

Nikolaos Evangeliou 18/12/2017 17:00

Deleted: SD

Nikolaos Evangeliou 18/12/2017 17:01

Deleted: 25.

Nikolaos Evangeliou 18/12/2017 17:01

Deleted: 15.8

Nikolaos Evangeliou 18/12/2017 17:04

Deleted: (

Nikolaos Evangeliou 18/12/2017 17:04

Deleted: ,

Nikolaos Evangeliou 18/12/2017 17:06

Deleted: Nevertheless, considering that the samples were not collected from the same regions exactly and at the same time, no safe conclusions can be obtained.

Nikolaos Evangeliou 18/12/2017 17:15

Deleted: Figure S 3

566 captures the temporal variation of the measured BC in snow. The RMSE was estimated to be
567 almost 63 ng g⁻¹, a relatively high value. The MFB of 47% indicates a strong overestimation
568 of snow concentrations, although in many samples the opposite was also observed (Figure S
569 3). This is in contrast to the previous data sets discussed, for which the model underestimated
570 measurements.

Nikolaos Evangeliou 18/12/2017 17:15
Deleted: Figure S 3

571 Further analysis was carried out to adequately understand the origin of the
572 aforementioned overestimations in the Canadian Arctic in both datasets (Doherty et al., 2010;
573 Macdonald et al., 2017), as they are shown to be rather systematic. For this reason, we have
574 calculated the average footprint emission sensitivities and the average BC contribution from
575 the major sources in ECLIPSE for the 2007 snow samples in the Canada Arctic and for Alert
576 samples. We have chosen these samples, because they were three or more times higher than
577 the observations and in this way we can locate the observed overestimations predicted with
578 FLEXPART (Figure 6).

Nikolaos Evangeliou 18/12/2017 17:15
Deleted: Figure 6

579 Regarding the model overestimation for the 2007 samples, the average footprint
580 emission sensitivity showed that the air was coming from continental regions of Canada with
581 a smaller contribution from Scandinavia (Figure 6). The highest emission sources for these
582 samples were TRA and DOM that contributed almost 80% to the snow concentrations,
583 whereas forest fires were less important at the time of sampling. Two hot spots were
584 identified, one along the borders of Canada with USA and another, of smaller intensity, in
585 southeastern Asia. A similar emission sensitivity was obtained for the same area of the
586 Canadian Arctic in 2009 only slightly shifted to the north; simulated concentrations were in
587 very good agreement with observations (Figure S 2). This shows that the model
588 overestimation for the 2007 samples is likely attributed to an overestimation of TRA and
589 DOM sources in North America in ECLIPSE for 2007. For the Alert samples, for which the
590 model strongly overestimated BC, the major sources were TRA and FLR, which contributed
591 55%, and BB which contributed about 7 ng g⁻¹ (22%) on average (Figure 6). Anthropogenic
592 BC arriving from Europe and Russia has been previously shown to be important for Alert air
593 pollutant concentrations (Sharma et al., 2013). The model overestimation of BC in snow
594 samples at Alert needs further investigation. It is likely that it originates from anthropogenic
595 emissions in northwestern America or in Europe, because forest fires in Canada and Russia,
596 although important for Alert (e.g., Qi et al., 2017), were not significant in the present
597 comparison.

Nikolaos Evangeliou 18/12/2017 17:15
Deleted: Figure 6

Nikolaos Evangeliou 18/12/2017 17:15
Deleted: Figure S 2

Nikolaos Evangeliou 18/12/2017 17:15
Deleted: Figure 6

603 4.2 Model deviation from snow EC measurements and region-specific 604 contribution of sources

605 It has been shown that measured concentrations of EC in snow in northwestern
606 European Russia and Western Siberia were underestimated in FLEXPART (Figure 2). This
607 was confirmed by the calculated fractional bias (see section 3.2), the spatial distribution of
608 which is shown in Figure S 1. To examine whether this underestimation was due to missing
609 emission sources or errors in modelled transport and deposition, we have calculated the
610 average footprint emission sensitivity for those sampling points, for which FLEXPART
611 strongly ($FB < -100\%$) and slightly ($-100\% < FB < 0\%$) underestimated the observed
612 values. The average footprint emission sensitivities are shown in Figure 7, together with the
613 locations of active fires in the last two months before the sample collection. The fire data
614 were adopted from MODIS (Moderate Resolution Imaging Spectroradiometer) (Giglio et al.,
615 2003) and the gas flaring facilities from the Global Gas Flaring Reduction Partnership
616 (GGFR) (<http://www.worldbank.org/en/programs/gasflaringreduction>).

617 When the model strongly underestimated the measured EC ($FB < -100\%$), the
618 average footprint emission sensitivity showed the highest values over the Yamal Peninsula
619 and the agglomeration of many gas flares in Khanty-Mansiysk (Figure 7, (b)). This might
620 confirm the finding of Huang et al. (2014) that gas flaring emissions in the ECLIPSE
621 inventory, while very high, are still underestimated. According to a related study by Huang
622 and Fu (2016), Russia contributes 57% to the global BC emissions from gas flaring.
623 Underestimation of modelled atmospheric concentrations compared to observations from the
624 Barents and Kara Seas was recently also reported by Popovicheva et al. (2017), although the
625 underestimation was relatively small.

626 When FLEXPART showed a moderate underestimation of EC concentrations in snow
627 ($-100\% < FB < 0\%$), the emission sensitivity was high near Arkhangelsk and over
628 Scandinavia (Figure 7). BC emissions in Scandinavia are considered relatively low in most
629 inventories and contribute no more than 6.5% to the global emissions in ACCMIP (Aerosol
630 Chemistry Climate Model Intercomparison Project) (Lamarque et al., 2013), 6.2% in
631 EDGARv4.2 (Emission Database for Global Atmospheric Research) (Olivier et al., 2005),
632 2.1% in MACCity (Monitoring Atmospheric Composition & Climate / megaCITY - Zoom for
633 the ENvironment) (Hollingsworth et al., 2008; Stein et al., 2012) and 3.3% in ECLIPSE
634 (Klimont et al., 2016). The highest emission sensitivity was found over northwestern Russia

Nikolaos Evangeliou 18/12/2017 17:15
Deleted: Figure 2

Nikolaos Evangeliou 18/12/2017 17:15
Deleted: Figure S 1

Nikolaos Evangeliou 18/12/2017 17:15
Deleted: Figure 7

Nikolaos Evangeliou 18/12/2017 17:15
Deleted: Figure 7

Nikolaos Evangeliou 18/12/2017 17:15
Deleted: Figure 7

640 | (Figure 7), a region which includes Murmansk. Pollution levels in Murmansk could be high
641 | due to emissions from local industry, mining, heating and transport (Law and Stohl, 2007).
642 | Another potential source region was Nenets/Komi area and Western Kazakhstan, where a few
643 | other flaring facilities are located (Figure 7).

Nikolaos Evangeliou 18/12/2017 17:15
Deleted: Figure 7

644 | Figure 7 shows that the underestimation of observed EC concentrations in snow
645 | strongly depends on the region, where samples are collected. In Western Siberia, the
646 | underestimation was larger than in northwestern European Russia. For this reason, we have
647 | computed the average region-specific emission sensitivities and the average region-specific
648 | contribution from the major polluting sources identified in ECLIPSE dataset. We distinguish
649 | between three regions, northwestern European Russia, Western Siberia (north of 62 °N) and
650 | Western Siberia (south of 62 °N) (Figure S 4–S 6). For the samples collected in northwestern
651 | European Russia (Figure S 4), an average contribution of 21.6 ng g⁻¹ from all sources was
652 | estimated to have originated mainly from TRA (7.7 ng g⁻¹) and DOM (10.4 ng g⁻¹) sources in
653 | Finland. The contribution from BB and FLR emissions was insignificant (8% and 6%,
654 | respectively), whereas the rest of the ECLIPSE sources were negligible (IND, ENE, WST).
655 | For the samples collected at high latitudes in Western Siberia, the average contribution from
656 | all sources was more than 4 times higher (86 ng g⁻¹) than those observed in northwestern
657 | European Russia (Figure S 5). FLR emissions accounted for 40% of the total contribution,
658 | which reflect the proximity of the sampling site to the main flaring facilities of Russia. The
659 | average contribution from TRA activities in Europe and southeastern Russia to the northern
660 | part of Western Siberia was 24%. Finally, DOM emissions in Eastern Europe also contributed
661 | another 28%. Finally, for the samples that were collected in the southern part of the Western
662 | Siberia an average contribution of 47.4 ng g⁻¹ was estimated from all sources included in
663 | ECLIPSE (Figure S 6). The highest contributing categories were TRA and DOM, whereas
664 | FLR appeared to contribute less, although the sampling site is close to Khanty-Mansiysk
665 | flaring region. This is attributed to the prevailing winds that forced flaring emissions to a
666 | northernmost direction opposite to the location of the sampling stations (see Figure S 6).

Nikolaos Evangeliou 18/12/2017 17:15
Deleted: Figure 7

Nikolaos Evangeliou 18/12/2017 17:15
Deleted: Figure 7

Nikolaos Evangeliou 18/12/2017 17:15
Deleted: Figure S 4

Nikolaos Evangeliou 18/12/2017 17:15
Deleted: Figure S 4

Nikolaos Evangeliou 18/12/2017 17:15
Deleted: Figure S 5

Nikolaos Evangeliou 18/12/2017 17:15
Deleted: Figure S 6

Nikolaos Evangeliou 18/12/2017 17:15
Deleted: Figure S 6

667 | Overall, the region-specific analysis of the sources contributing to modelled BC in
668 | snow showed that the DOM, FLR and/or TRA sources might explain the model
669 | underestimation in high Arctic. However, in the most recent assessments of BC of the higher
670 | Arctic (Popovicheva et al., 2017; Winiger et al., 2017), it was shown that ECLIPSE captures
671 | levels of BC quite well, whereas FLR emissions might have a smaller impact in the Central
672 | Siberian Arctic (Tiksi) than previously estimated. Surprisingly, the average contribution from

681 | BB in lower latitudes was extremely low in all Western Siberia (Figure S 5 and S 6), despite
682 | the fact that sampling took place in springtime, where BB becomes important. Evangeliou et
683 | al. (2016) reported that using a different dataset, that is based on the same approach as GFED,
684 | but includes updated emission factors for Eurasia, surface concentrations of BC in the Arctic
685 | stations can be substantially higher. This shows the need for further investigation of BC
686 | sources in the Russian Arctic.

Nikolaos Evangeliou 18/12/2017 17:15

Deleted: Figure S 5

687 | 5 Conclusions

688 | We have analysed snow samples collected in Western Siberia and northwestern
689 | European Russia in 2014, 2015 and 2016 with respect to EC. This region is of major interest
690 | due to its large uncertainty in BC emissions and because it is located in the main transport
691 | route of BC to the Arctic. An effort to constrain the sources that contribute to measured
692 | concentration in BC in snow was made using the LPDM FLEXPART (version 10).

693 | The observed EC levels in snow varied widely within and between regions (3–219 ng g⁻¹
694 | for 2014, 46–175 ng g⁻¹ in 2015 and 7–161 ng g⁻¹ in 2016), and are in the upper range of
695 | previously reported concentrations of EC and BC in snow in the Arctic region. However, the
696 | observed levels presented here appear typical for Western Siberia, which is subject to high
697 | domestic Russian emissions as well as to transport from distant European ones.

698 | The snow BC concentrations predicted by the model are in a fair agreement with EC
699 | observations over Western Siberia and northwestern European Russia ($R = 0.5 - 0.8$).
700 | However, the calculated negative MFB values (-48% to -27%) showed that the model
701 | systematically underestimated observations in Russia. This underestimation strongly
702 | depended on the region where the samples were collected. In northwestern European Russia,
703 | the main contributing sources were TRA and DOM mainly from adjacent regions in Finland.
704 | TRA and DOM contributed double to snow BC sampled at low latitudes of Western Siberia
705 | (<60°N) as compared to samples collected over regions above 60°N; the majority of these
706 | emissions originating from highly populated centres in Central Europe. Finally, in higher
707 | latitudes of Western Siberia (>60°N), snow BC concentrations were further increased mainly
708 | due to FLR emissions from facilities located close to the snow sampling points.

709 | The modelled BC concentrations in snow were further investigated using two
710 | independent public measurement datasets that include samples from all over the Arctic for the
711 | period 2005 to 2009 and from Alert in 2014 and 2015. The model captured levels of BC fairly

713 well despite the large variation in measured concentrations. An exception was observed in
714 North America in spring 2007 and in Alert observatory in late winter – early spring 2015. In
715 both cases, the major sources were along the Canadian borders with USA and in Western
716 Europe. Considering the fact that similar deviations were not observed in samples collected in
717 the area during other years, it is likely that some of the prevailing sources of BC in this region
718 show strong temporal variability in their emissions, and this is not taken into account in
719 ECLIPSE inventory. Previously reported average measurements of BC concentrations in
720 snow in Western Siberia and northwestern European Russia were 80 ± 43 ng g⁻¹, which is
721 about 30% higher than the EC measurements presented here (50 ± 46 ng g⁻¹).

722 **Data availability.** All data used for the present publication can be obtained from the
723 corresponding author upon request.

724 **Competing interests.** The authors declare that they have no conflict of interest.

725 **Acknowledgements.** We would like to acknowledge the project entitled “Emissions of
726 Short-Lived Climate Forcers near and in the Arctic (SLICFONIA)”, which was funded by the
727 NORRUSS research program of the Research Council of Norway (Project ID: 233642) and
728 the Russian Fund for Basic Research (project No. 15-05-08374) for funding snow sampling in
729 the White Sea catchment area. We also thank Sergey Belorukov, Andrey Boev, Anton
730 Bulokhov, Victor Drozdov, Sergey Kirpotin, Ivan Kritzkov, Rinat Manasypov, Ivan
731 Semenyuk, and Alexander Yakovlev for helping during the three expeditions and
732 Academician Alexander P. Lisitzin for his valuable recommendations. O. S. Pokrovsky and S.
733 N. Vorobiev acknowledge support from BIO-GEO-CLIM grant No 14.B25.31.0001 for
734 sampling in Western Siberia. Acknowledgements are also owed to IIASA (especially Chris
735 Heyes and Zig Klimont) for providing the BC emission dataset. Computational and storage
736 resources for the FLEXPART simulations have been provided by NOTUR (NN9419K) and
737 NORSTORE (NS9419K). All plots from FLEXPART simulations have been included in an
738 interactive website for fast visualization
739 (http://niflheim.nilu.no/NikolaosPY/SnowBC_141516.py). All results can be accessed upon
740 request to the corresponding author of this manuscript.

741 **Author Contributions.** N. Evangeliou designed and performed the modelling experiments
742 and wrote the paper. V. P. Shevchenko organised and performed the sampling of EC, K.-E.
743 Yttri performed all the TOA of the snow samples. S. Eckhardt modified FLEXPART model
744 for the calculation of footprint emission sensitivities for deposited mass. E. Sollum wrote an

Nikolaos Evangeliou 18/12/2017 17:13

Deleted: 101

Nikolaos Evangeliou 18/12/2017 17:13

Deleted: 15

Nikolaos Evangeliou 18/12/2017 17:13

Deleted: 20

Nikolaos Evangeliou 18/12/2017 17:13

Deleted: 83

Nikolaos Evangeliou 18/12/2017 17:13

Deleted: 37

750 algorithm that computes the starting date of the FLEXPART releases based on the water
751 equivalent volume from ECMWF. O. S. Pokrovsky, V. O. Kobelev, V. B. Korobov, A. A.
752 Lobanov, D. P. Starodymova and S. N. Vorobiev assisted the sampling campaigns in Western
753 Siberia and northwestern European Russia during 2014–2016. R. L. Thompson and A. Stohl
754 supervised the study and wrote parts of the paper.

755

756 **References**

- 757 Aamaas, B., Bøggild, C. E., Stordal, F., Berntsen, T., Holmén, K. and Ström, J.: Elemental
758 carbon deposition to Svalbard snow from Norwegian settlements and long-range transport,
759 *Tellus, Ser. B Chem. Phys. Meteorol.*, 63(3), 340–351, doi:10.1111/j.1600-
760 0889.2011.00531.x, 2011.
- 761 AMAP: AMAP assessment 2015: Black carbon and ozone as Arctic climate forciers, Arctic
762 Monitoring and Assessment Programme (AMAP), Oslo, Norway., 2015.
- 763 Andreae, M. O. and Gelencsér, A.: Black carbon or brown carbon? The nature of light-
764 absorbing carbonaceous aerosols, *Atmos. Chem. Phys.*, 6(3), 3419–3463, doi:10.5194/acpd-6-
765 3419-2006, 2006.
- 766 Bond, T. C., Streets, D. G., Yarber, K. F., Nelson, S. M., Woo, J. H. and Klimont, Z.: A
767 technology-based global inventory of black and organic carbon emissions from combustion, *J.*
768 *Geophys. Res. D Atmos.*, 109(14), 1–43, doi:10.1029/2003JD003697, 2004.
- 769 Bond, T. C., Doherty, S. J., Fahey, D. W., Forster, P. M., Berntsen, T., Deangelo, B. J.,
770 Flanner, M. G., Ghan, S., Kärcher, B., Koch, D., Kinne, S., Kondo, Y., Quinn, P. K., Sarofim,
771 M. C., Schultz, M. G., Schulz, M., Venkataraman, C., Zhang, H., Zhang, S., Bellouin, N.,
772 Guttikunda, S. K., Hopke, P. K., Jacobson, M. Z., Kaiser, J. W., Klimont, Z., Lohmann, U.,
773 Schwarz, J. P., Shindell, D., Storelvmo, T., Warren, S. G. and Zender, C. S.: Bounding the
774 role of black carbon in the climate system: A scientific assessment, *J. Geophys. Res. Atmos.*,
775 118(11), 5380–5552, doi:10.1002/jgrd.50171, 2013.
- 776 Brandt, R. E., Warren, S. G., Worby, A. P. and Grenfell, T. C.: Surface albedo of the
777 Antarctic sea ice zone, *J. Clim.*, 18(17), 3606–3622, doi:10.1175/JCLI3489.1, 2005.
- 778 Cavalli, F., Viana, M., Yttri, K. E., Genberg, J. and Putaud, J.-P.: Toward a standardised
779 thermal-optical protocol for measuring atmospheric organic and elemental carbon: the

780 EUSAAR protocol, *Atmos. Meas. Tech.*, 3(1), 79–89, doi:10.5194/amt-3-79-2010, 2010.

781 Cavalli, F., Putaud, J.-P. and Yttri, K. E.: Availability and quality of the EC and OC
782 measurements within EMEP, including results of the fifth interlaboratory comparison of
783 analytical methods for carbonaceous particulate matter within EMEP (2012), 2015.

784 Clarke, A. D. and Noone, K. J.: Soot in the arctic snowpack: a cause for perturbations in
785 radiative transfer, *Atmos. Environ.*, 41(SUPPL.), 64–72, doi:10.1016/0004-6981(85)90113-1,
786 1985.

787 Doherty, S. J., Warren, S. G., Grenfell, T. C., Clarke, A. D. and Brandt, R. E.: Light-
788 absorbing impurities in Arctic snow, *Atmos. Chem. Phys.*, 10(23), 11647–11680,
789 doi:10.5194/acp-10-11647-2010, 2010.

790 Doherty, S. J., Grenfell, T. C., Forsström, S., Hegg, D. L., Brandt, R. E. and Warren, S. G.:
791 Observed vertical redistribution of black carbon and other insoluble light-absorbing particles
792 in melting snow, *J. Geophys. Res. Atmos.*, 118(11), 5553–5569, doi:10.1002/jgrd.50235,
793 2013.

794 Eckhardt, S., Cassiani, M., Evangeliou, N., Sollum, E., Pisso, I. and Stohl, A.: Source-
795 receptor matrix calculation for deposited mass with the Lagrangian particle dispersion model
796 FLEXPART v10.2 in backward mode, *Geosci. Model Dev.*, 10, 4605–4618,
797 doi:10.5194/gmd-10-4605-2017, 2017.

798 Evangeliou, N., Balkanski, Y., Hao, W. M., Petkov, A., Silverstein, R. P., Corley, R.,
799 Nordgren, B. L., Urbanski, S. P., Eckhardt, S., Stohl, A., Tunved, P., Crepinsek, S., Jefferson,
800 A., Sharma, S., Nøjgaard, J. K. and Skov, H.: Wildfires in northern Eurasia affect the budget
801 of black carbon in the Arctic—a 12-year retrospective synopsis (2002–2013), *Atmos. Chem.*
802 *Phys.*, 16(12), 7587–7604, doi:10.5194/acp-16-7587-2016, 2016.

803 Flanner, M. G., Zender, C. S., Randerson, J. T. and Rasch, P. J.: Present-day climate forcing
804 and response from black carbon in snow, *J. Geophys. Res. Atmos.*, 112(11), 1–17,
805 doi:10.1029/2006JD008003, 2007.

806 Forsström, S., Isaksson, E., Skeie, R. B., Ström, J., Pedersen, C. A., Hudson, S. R., Berntsen,
807 T. K., Lihavainen, H., Godtliebsen, F. and Gerland, S.: Elemental carbon measurements in
808 European Arctic snow packs, *J. Geophys. Res. Atmos.*, 118(24), 13614–13627,
809 doi:10.1002/2013JD019886, 2013.

810 Forster, C., Wandering, U., Wotawa, G., James, P., Mattis, I., Althausen, D., Simmonds, P.,
811 O'Doherty, S., Jennings, S. G., Kleefeld, C., Schneider, J., Trickl, T., Kreipl, S., Jäger, H. and
812 Stohl, A.: Transport of boreal forest fire emissions from Canada to Europe, *J. Geophys. Res.*,
813 106, 22887, doi:10.1029/2001JD900115, 2001.

814 Giglio, L., Descloitres, J., Justice, C. O. and Kaufman, Y. J.: An enhanced contextual fire
815 detection algorithm for MODIS, *Remote Sens. Environ.*, 87(2–3), 273–282,
816 doi:10.1016/S0034-4257(03)00184-6, 2003.

817 Giglio, L., Randerson, J. T. and van der Werf, G. R.: Analysis of daily, monthly, and annual
818 burned area using the fourth-generation global fire emissions database (GFED4), *J. Geophys.*
819 *Res. Biogeosciences*, 118, 317–328, doi:10.1002/jgrg.20042, 2013, 2013.

820 Grythe, H., Kristiansen, N. I., Groot Zwaafink, C. D., Eckhardt, S., Ström, J., Tunved, P.,
821 Krejci, R. and Stohl, A.: A new aerosol wet removal scheme for the Lagrangian particle
822 model FLEXPARTv10, *Geosci. Model Dev.*, 10, 1447–1466, doi:10.5194/gmd-10-1447-
823 2017, 2017.

824 Hadley, O. L., Corrigan, C. E., Kirchstetter, T. W., Cliff, S. S. and Ramanathan, V.: Measured
825 black carbon deposition on the Sierra Nevada snow pack and implication for snow pack
826 retreat, *Atmos. Chem. Phys.*, 10(15), 7505–7513, doi:10.5194/acp-10-7505-2010, 2010.

827 Hansen, J. and Nazarenko, L.: Soot climate forcing via snow and ice albedos, *Proc. Natl.*
828 *Acad. Sci. U. S. A.*, 101(2), 423–428, doi:10.1073/pnas.2237157100, 2004.

829 Hao, W. M., Petkov, A., Nordgren, B. L., Silverstein, R. P., Corley, R. E., Urbanski, S. P.,
830 Evangeliou, N., Balkanski, Y. and Kinder, B.: Daily black carbon emissions from fires in
831 Northern Eurasia from 2002 to 2013, *Geosci. Model Dev. Discuss.*, (April), 1–24,
832 doi:10.5194/gmd-2016-89, 2016.

833 Hegg, D. A., Warren, S. G., Grenfell, T. C., Doherty, S. J., Larson, T. V. and Clarke, A. D.:
834 Source attribution of black carbon in arctic snow, *Environ. Sci. Technol.*, 43(11), 4016–4021,
835 doi:10.1021/es803623f, 2009.

836 Hegg, D. A., Warren, S. G., Grenfell, T. C., Doherty, S. J. and Clarke, A. D.: Sources of light-
837 absorbing aerosol in arctic snow and their seasonal variation, *Atmos. Chem. Phys.*, 10(22),
838 10923–10938, doi:10.5194/acp-10-10923-2010, 2010.

839 Hollingsworth, A., Engelen, R. J., Textor, C., Benedetti, A., Boucher, O., Chevallier, F.,
840 Dethof, A., Elbern, H., Eskes, H., Flemming, J., Granier, C., Kaiser, J. W., Morcrette, J. J.,
841 Rayner, P., Peuch, V. H., Rouil, L., Schultz, M. G. and Simmons, A. J.: Toward a monitoring
842 and forecasting system for atmospheric composition: The GEMS project, *Bull. Am. Meteorol.*
843 *Soc.*, 89(8), 1147–1164, doi:10.1175/2008BAMS2355.1, 2008.

844 Huang, K. and Fu, J. S.: Data Descriptor : A global gas flaring black carbon emission rate
845 dataset from 1994 to 2012, *Nature*, 1–11, doi:10.1038/sdata.2016.104, 2016.

846 Huang, K., Fu, J. S., Hodson, E. L., Dong, X., Cresko, J., Prikhodko, V. Y., Storey, J. M. and
847 Cheng, M. D.: Identification of missing anthropogenic emission sources in Russia:
848 Implication for modeling arctic haze, *Aerosol Air Qual. Res.*, 14(7), 1799–1811,
849 doi:10.4209/aaqr.2014.08.0165, 2014.

850 Ingvander, S., Rosqvist, G., Svensson, J. and Dahlke, H. E.: Seasonal and interannual
851 variability of elemental carbon in the snowpack of Storglaci??ren, northern Sweden, *Ann.*
852 *Glaciol.*, 54(62), 50–58, doi:10.3189/2013AoG62A229, 2013.

853 Jankowski, N., Schmidl, C., Marr, I. L., Bauer, H. and Puxbaum, H.: Comparison of methods
854 for the quantification of carbonate carbon in atmospheric PM10 aerosol samples, *Atmos.*
855 *Environ.*, 42(34), 8055–8064, doi:10.1016/j.atmosenv.2008.06.012, 2008.

856 Klimont, Z., Kupiainen, K., Heyes, C., Purohit, P., Cofala, J., Rafaj, P., Borken-Kleefeld, J.
857 and Schöpp, W.: Global anthropogenic emissions of particulate matter including black
858 carbon, *Atmos. Chem. Phys. Discuss.*, (October), 1–72, doi:10.5194/acp-2016-880, 2016.

859 Lamarque, J. F., Shindell, D. T., Josse, B., Young, P. J., Cionni, I., Eyring, V., Bergmann, D.,
860 Cameron-Smith, P., Collins, W. J., Doherty, R., Dalsoren, S., Faluvegi, G., Folberth, G.,
861 Ghan, S. J., Horowitz, L. W., Lee, Y. H., MacKenzie, I. A., Nagashima, T., Naik, V.,
862 Plummer, D., Righi, M., Rumbold, S. T., Schulz, M., Skeie, R. B., Stevenson, D. S., Strode,
863 S., Sudo, K., Szopa, S., Voulgarakis, A. and Zeng, G.: The atmospheric chemistry and climate
864 model intercomparison Project (ACCMIP): Overview and description of models, simulations
865 and climate diagnostics, *Geosci. Model Dev.*, 6(1), 179–206, doi:10.5194/gmd-6-179-2013,
866 2013.

867 Law, K. S. and Stohl, A.: Arctic Air Pollution: Origins and Impacts, *Science* (80-.),
868 315(5818), 1537–1540, doi:10.1126/science.1137695, 2007.

869 Lelieveld, J., Evans, J. S., Fnais, M., Giannadaki, D. and Pozzer, A.: The contribution of
870 outdoor air pollution sources to premature mortality on a global scale., *Nature*, 525(7569),
871 367–71, doi:10.1038/nature15371, 2015.

872 Liu, J., Fan, S., Horowitz, L. W. and Levy, H.: Evaluation of factors controlling long-range
873 transport of black carbon to the Arctic, *J. Geophys. Res.*, 116(D4), D04307,
874 doi:10.1029/2010JD015145, 2011.

875 Macdonald, K. M., Sharma, S., Toom, D., Chivulescu, A., Hanna, S., Bertram, A., Platt, A.,
876 Elsasser, M., Huang, L., Chellman, N., McConnell, J. R., Bozem, H., Kunkel, D., Lei, Y. D.,
877 Evans, G. J. and Abbatt, J. P. D.: Observations of Atmospheric Chemical Deposition to High
878 Arctic Snow, *Atmos. Chem. Phys.*, 17, 5775–5788, doi:10.5194/acp-17-5775-2017, 2017.

879 McConnell, J. R., Edwards, R., Kok, G. L., Flanner, M. G., Zender, C. S., Saltzman, E. S.,
880 Banta, J. R., Pasteris, D. R., Carter, M. M. and Kahl, J. D. W.: 20th-Century Industrial Black
881 Carbon Emissions Altered Arctic Climate Forcing, *Science* (80-.), 317(5843), 1381–1384,
882 doi:10.1126/science.1144856, 2007.

883 Ogren, J. A., Charlson, R. J. and Groblicki, P. J.: Determination of elemental carbon in
884 rainwater, *Anal. Chem.*, 55(9), 1569–1572, doi:10.1021/ac00260a027, 1983.

885 Olivier, J. G. J., Aardenne, J. A. Van, Dentener, F. J., Pagliari, V., Ganzeveld, L. N. and
886 Peters, J. A. H. W.: Recent trends in global greenhouse gas emissions: regional trends 1970–
887 2000 and spatial distribution of key sources in 2000, *Environ. Sci.*, 2(2–3), 81–99,
888 doi:10.1080/15693430500400345, 2005.

889 Petzold, A., Ogren, J. A., Fiebig, M., Laj, P., Li, S. M., Baltensperger, U., Holzer-Popp, T.,
890 Kinne, S., Pappalardo, G., Sugimoto, N., Wehrli, C., Wiedensohler, A. and Zhang, X. Y.:
891 Recommendations for reporting black carbon measurements, *Atmos. Chem. Phys.*, 13(16),
892 8365–8379, doi:10.5194/acp-13-8365-2013, 2013.

893 Popovicheva, O. B., Evangelidou, N., Eleftheriadis, K., Kalogridis, A. C., Movchan, V.,
894 Sitnikov, N., Eckhardt, S., Makshtas, A. and Stohl, A.: Black carbon sources constrained by
895 observations and modeling in the Russian high Arctic, *Environ. Sci. Technol.*, submitted,
896 doi:10.1021/acs.est.6b05832, 2017.

897 Qi, L., Li, Q., Henze, D. K., Tseng, H.-L. and He, C.: Sources of Springtime Surface Black
898 Carbon in the Arctic: An Adjoint Analysis, *Atmos. Chem. Phys. Discuss.*, (February), 1–32,

899 doi:10.5194/acp-2016-1112, 2017.

900 Ruppel, M. M., Isaksson, I., Ström, J., Beaudon, E., Svensson, J., Pedersen, C. A. and
901 Korhola, A.: Increase in elemental carbon values between 1970 and 2004 observed in a 300-
902 year ice core from Holtedahlfonna (Svalbard), *Atmos. Chem. Phys.*, 14(20), 11447–11460,
903 doi:10.5194/acp-14-11447-2014, 2014.

904 Sand, M., Berntsen, T. K., von Salzen, K., Flanner, M. G., Langner, J. and Victor, D. G.:
905 Response of Arctic temperature to changes in emissions of short-lived climate forcers, *Nat.*
906 *Clim. Chang.*, 6(November), 1–5, doi:10.1038/nclimate2880, 2015.

907 Seibert, P. and Frank, A.: Source-receptor matrix calculation with a Lagrangian particle
908 dispersion model in backward mode, *Atmos. Chem. Phys.*, 4(1), 51–63, doi:10.5194/acp-4-
909 51-2004, 2004.

910 Sharma, S., Ishizawa, M., Chan, D., Lavoué, D., Andrews, E., Eleftheriadis, K. and
911 Maksyutov, S.: 16-year simulation of arctic black carbon: Transport, source contribution, and
912 sensitivity analysis on deposition, *J. Geophys. Res. Atmos.*, 118(2), 943–964,
913 doi:10.1029/2012JD017774, 2013.

914 Shiraiwa, M., Kondo, Y., Moteki, N., Takegawa, N., Sahu, L. K., Takami, A., Hatakeyama,
915 S., Yonemura, S. and Blake, D. R.: Radiative impact of mixing state of black carbon aerosol
916 in Asian outflow, *J. Geophys. Res. Atmos.*, 113(24), 1–13, doi:10.1029/2008JD010546, 2008.

917 Silverstein, J. C., Parsad, N. M. and Tsirline, V.: NIH Public Access, , 41(6), 927–935,
918 doi:10.1016/j.jbi.2008.02.008.Automatic, 2009.

919 Singh, P. and Haritashya, U. K.: *Encyclopedia of Snow, Ice and Glaciers.*, 2011.

920 Slinn, W. G. N.: Predictions for particle deposition to vegetative canopies, *Atmos. Environ.*,
921 16, 1785–1794, doi:10.1016/0004-6981(82)90271-2, 1982.

922 Stein, O., Flemming, J., Inness, A., Kaiser, J. W. and Schultz, M. G.: Global reactive gases
923 forecasts and reanalysis in the MACC project, *J. Integr. Environ. Sci.*, 8168(October 2014),
924 1–14, doi:10.1080/1943815X.2012.696545, 2012.

925 Stohl, A., Hittenberger, M. and Wotawa, G.: Validation of the lagrangian particle dispersion
926 model FLEXPART against large-scale tracer experiment data, *Atmos. Environ.*, 32(24),
927 4245–4264, doi:10.1016/S1352-2310(98)00184-8, 1998.

928 Stohl, A., Forster, C., Eckhardt, S., Spichtinger, N., Huntrieser, H., Heland, J., Schlager, H.,
929 Wilhelm, S., Arnold, F. and Cooper, O.: A backward modeling study of intercontinental
930 pollution transport using aircraft measurements, *J. Geophys. Res. Atmos.*, 108(D12), 4370,
931 doi:10.1029/2002JD002862, 2003.

932 Stohl, A., Forster, C., Frank, A., Seibert, P. and Wotawa, G.: Technical note: The Lagrangian
933 particle dispersion model FLEXPART version 6.2, *Atmos. Chem. Phys.*, 5(9), 2461–2474,
934 doi:10.5194/acp-5-2461-2005, 2005.

935 Stohl, A., Andrews, E., Burkhardt, J. F., Forster, C., Herber, A., Hoch, S. W., Kowal, D.,
936 Lunder, C., Mefford, T., Ogren, J. A., Sharma, S., Spichtinger, N., Stebel, K., Stone, R.,
937 Ström, J., Tørseth, K., Wehrli, C. and Yttri, K. E.: Pan-Arctic enhancements of light
938 absorbing aerosol concentrations due to North American boreal forest fires during summer
939 2004, *J. Geophys. Res. Atmos.*, 111(22), 1–20, doi:10.1029/2006JD007216, 2006.

940 Stohl, A., Klimont, Z., Eckhardt, S., Kupiainen, K., Shevchenko, V. P., Kopeikin, V. M. and
941 Novigatsky, A. N.: Black carbon in the Arctic: The underestimated role of gas flaring and
942 residential combustion emissions, *Atmos. Chem. Phys.*, 13(17), 8833–8855, doi:10.5194/acp-
943 13-8833-2013, 2013.

944 Stohl, A., Aamaas, B., Amann, M., Baker, L. H., Bellouin, N., Bernsten, T. K., Boucher, O.,
945 Cherian, R., Collins, W., Daskalakis, N., Dusinska, M., Eckhardt, S., Fuglestvedt, J. S., Harju,
946 M., Heyes, C., Hodnebrog, Hao, J., Im, U., Kanakidou, M., Klimont, Z., Kupiainen, K., Law,
947 K. S., Lund, M. T., Maas, R., MacIntosh, C. R., Myhre, G., Myriokefalitakis, S., Olivié, D.,
948 Quaas, J., Quennehen, B., Raut, J. C., Rumbold, S. T., Samset, B. H., Schulz, M., Seland,
949 Shine, K. P., Skeie, R. B., Wang, S., Yttri, K. E. and Zhu, T.: Evaluating the climate and air
950 quality impacts of short-lived pollutants, *Atmos. Chem. Phys.*, 15(18), 10529–10566,
951 doi:10.5194/acp-15-10529-2015, 2015.

952 Svensson, J., Ström, J., Hansson, M., Lihavainen, H. and Kerminen, V.-M.: Observed metre
953 scale horizontal variability of elemental carbon in surface snow, *Environ. Res. Lett.*, 8(3),
954 34012, doi:10.1088/1748-9326/8/3/034012, 2013.

955 Turner, M. D., Henze, D. K., Capps, S. L., Hakami, A., Zhao, S., Resler, J., Carmichael, G.
956 R., Stanier, C. O., Baek, J., Sandu, A., Russell, A. G., Nenes, A., Pinder, R. W., Napelenok, S.
957 L., Bash, J. O., Percell, P. B. and Chai, T.: Premature deaths attributed to source-specific BC
958 emissions in six urban US regions, , 10(114014), doi:10.1088/1748-9326/10/11/114014/meta,

959 2005.

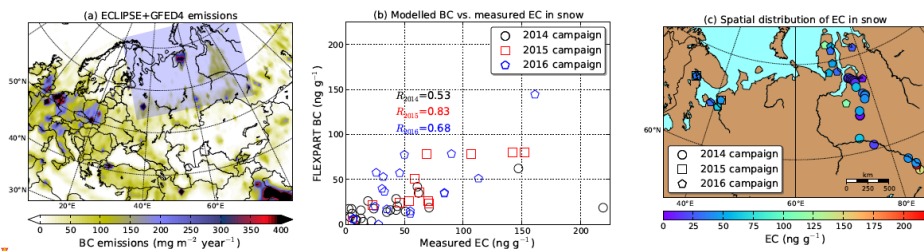
960 Wang, Q., Jacob, D. J., Fisher, J. A., Mao, J., Leibensperger, E. M., Carouge, C. C., Le Sager,
961 P., Kondo, Y., Jimenez, J. L., Cubison, M. J. and Doherty, S. J.: Sources of carbonaceous
962 aerosols and deposited black carbon in the Arctic in winter-spring: Implications for radiative
963 forcing, *Atmos. Chem. Phys.*, 11(23), 12453–12473, doi:10.5194/acp-11-12453-2011, 2011.

964 Warren, S. G. and Wiscombe, W. J.: A Model for the Spectral Albedo of Snow. II: Snow
965 Containing Atmospheric Aerosols, *J. Atmos. Sci.*, 37, 2734–2745, doi:10.1175/1520-
966 0469(1980)037<2734:AMFTSA>2.0.CO;2, 1980.

967 Winiger, P., Andersson, A., Eckhardt, S., Stohl, A., Semiletov, I. P., Dudarev, O. V., Charkin,
968 A., Shakhova, N., Klimont, Z., Heyes, C. and Gustafsson, Ö.: Siberian Arctic black carbon
969 sources constrained by model and observation, *Proc. Natl. Acad. Sci.*, 1–8,
970 doi:10.1073/pnas.1613401114, 2017.

971

973



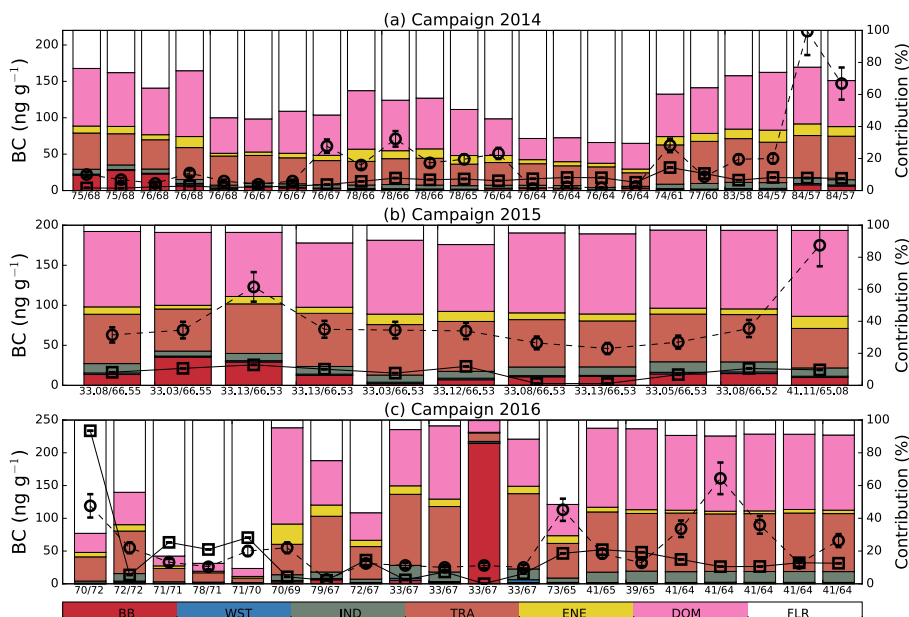
974 **Figure 1.** (a) Total emissions of BC (anthropogenic emissions from ECLIPSE (Klimont et al.,
 975 2016) and biomass burning from GFED4 (Giglio et al., 2013). The blue shade shows the area
 976 of interest that is zoomed on the right. (b) Comparison of modelled BC concentrations in
 977 snow with measured EC concentrations. (c) Spatial distribution of EC in snow measured by
 978 thermal optical analysis (TOA) of filtered snow samples from northwestern European Russia
 979 and Western Siberia in spring–time 2014, 2015 and 2016 (Silverstein et al., 2009).

980

Nikolaos Evangeliou 18/12/2017 14:30

Deleted:
 Unknown
Formatted: Font:Times New Roman, 12 pt, Bold

SOURCE CONTRIBUTION TO SNOW BC

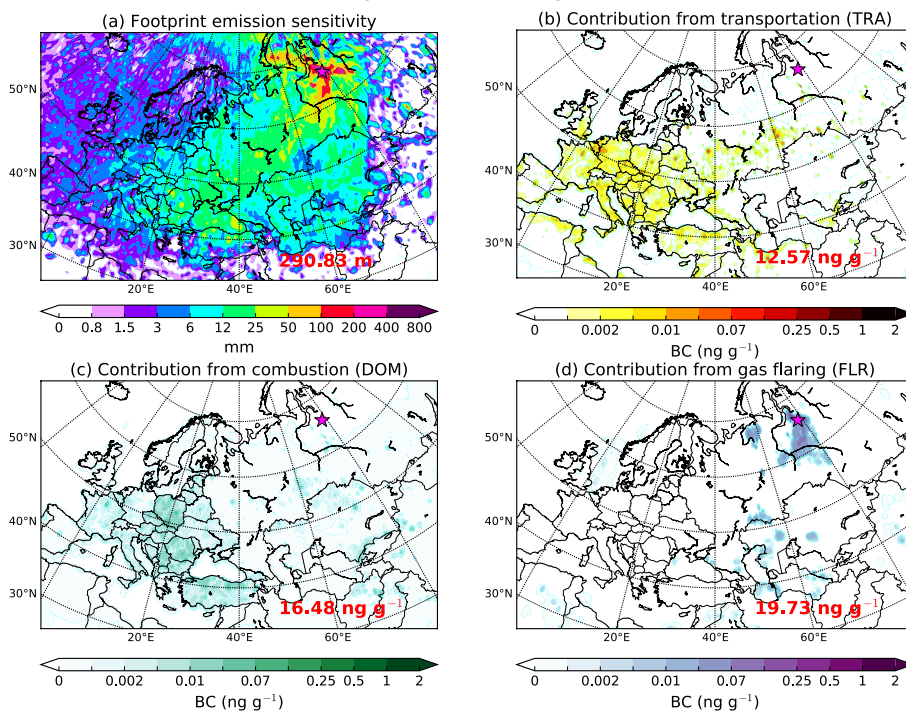


982

983 **Figure 2.** Contribution from the various emission categories considered in the ECLIPSE and
 984 GFED inventories to simulated BC concentrations in snow in (a) 2014, (b) 2015 and (c) 2016
 985 in Western Siberia and northwestern European Russia. BB stands for biomass burning, WST
 986 for waste burning, IND for industrial combustion and processing, TRA for surface
 987 transportation, ENE for emissions from energy conversion, and extraction, DOM for
 988 residential and commercial combustion, and FLR for gas flaring. Bars show the relative
 989 source contribution (0 –100%, right axis) and are sorted, from left to right, from the
 990 northernmost to the southernmost measurement location (coordinates are reported on the
 991 bottom as longitude/latitude). Measured EC concentrations in snow are reported with open
 992 circles, whereas modelled BC is shown with open rectangles (left axis).

993

**EMISSION SENSITIVITY AND SOURCE CONTRIBUTION TO SNOW BC IN 2014
(78.17° E - 65.78° N)**

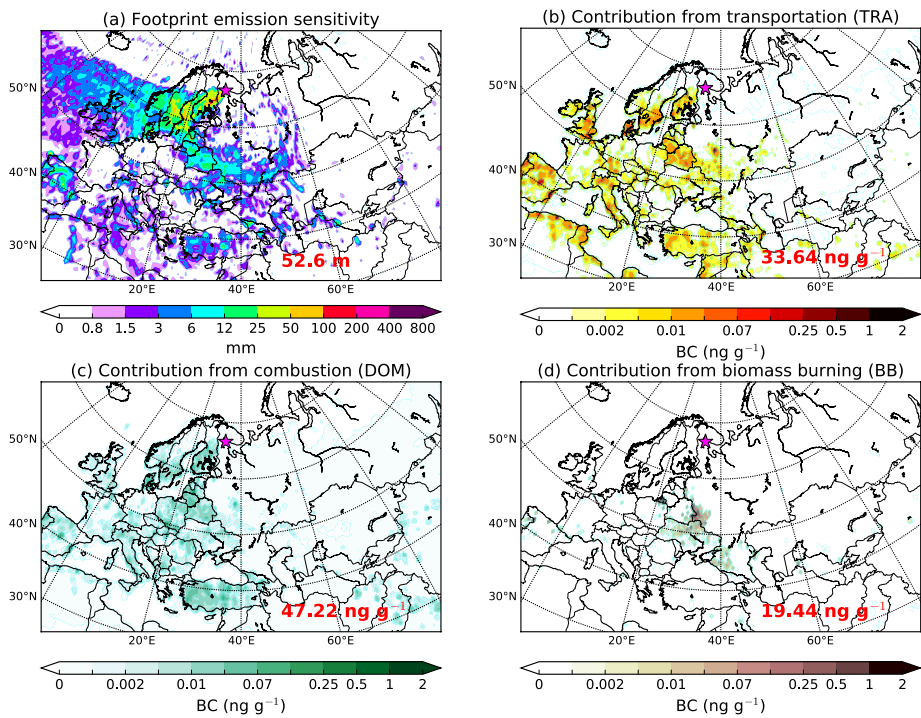


994

995 **Figure 3.** (a) FLEXPART emission sensitivity, contribution from (b) transportation (TRA),
 996 (c) residential and commercial combustion (DOM) and (d) gas flaring (FLR) to the maximum
 997 measured concentration of snow EC recorded along the transect from Tomsk to Yamal
 998 Peninsula in Western Siberia during the campaign of 2014.

999

**EMISSION SENSITIVITY AND SOURCE CONTRIBUTION TO SNOW BC IN 2015
(33.13° E - 66.53° N)**

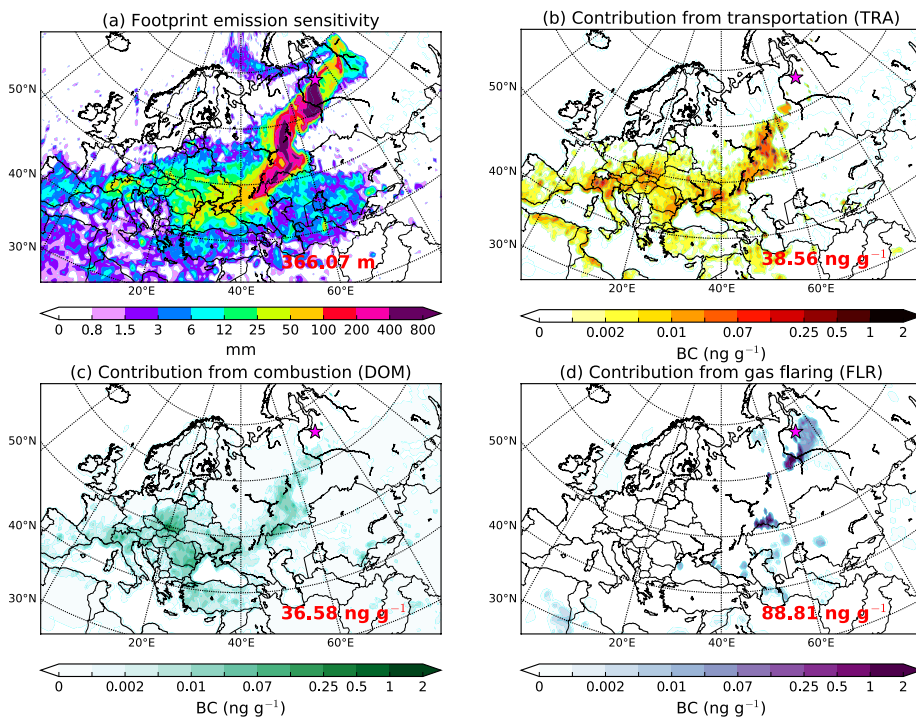


1000

1001 **Figure 4.** (a) FLEXPART emission sensitivity, (b) contribution from transportation (TRA),
 1002 (c) residential and commercial combustion (DOM) and (d) gas flaring (FLR) to the maximum
 1003 measured concentration of snow EC recorded in northwestern European Russia (Kindo
 1004 Peninsula and Arkhangelsk region) during the campaign of 2015.

1005

**EMISSION SENSITIVITY AND SOURCE CONTRIBUTION TO SNOW BC IN 2016
(72.94° E - 65.36° N)**

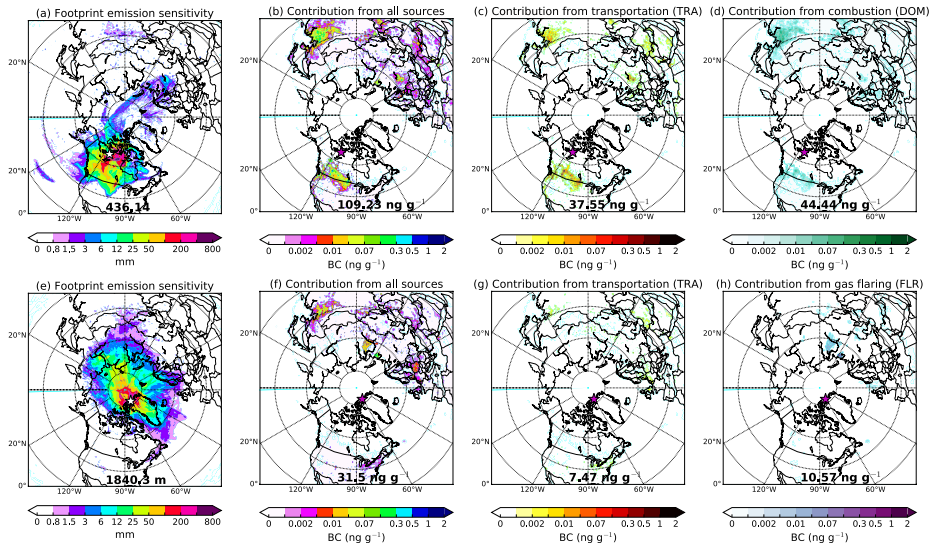


1006

1007 **Figure 5.** (a) FLEXPART emission sensitivity and (b) contribution from transportation
 1008 (TRA), (c) residential and commercial combustion (DOM) and (d) gas flaring (FLR) to the
 1009 maximum measured concentration of snow EC recorded in Kindo Peninsula, Arkhangelsk and
 1010 Yamal Peninsula (northwestern European Russia, Western Siberia) during the campaign of
 1011 2016.

1012

**EMISSION SENSITIVITY AND SOURCE CONTRIBUTION TO SNOW BC
(CANADIAN ARCTIC 2007 - ALERT 2014-2015)**

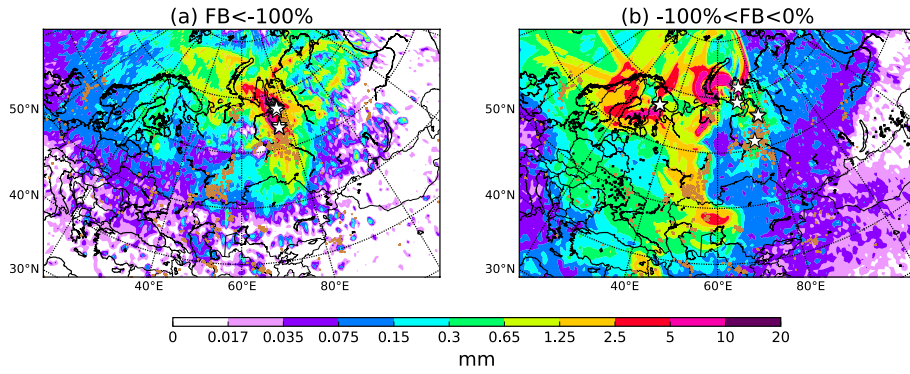


1013

1014 **Figure 6.** (a–d) Footprint emission sensitivity and major contribution from all sources, TRA
 1015 and DOM averaged for the samples that showed overestimated modelled concentrations of
 1016 BC in 2007 (Doherty et al., 2010). (e–h) Footprint emission sensitivity and contribution from
 1017 all sources, TRA and FLR for the samples collected in Alert (Macdonald et al., 2017) that
 1018 model overestimated by more than three times.

1019

**AVERAGE FOOTPRINT EMISSION SENSITIVITY
NORMALISED AGAINST UNDERESTIMATION FROM OBSERVATIONS**



1020

1021 **Figure 7.** (a) Footprint emission sensitivity from FLEXPART averaged for the sampling
1022 points where the model underestimated observations significantly ($FB < -100\%$) and (b)
1023 less significantly ($-100\% < FB < 0\%$). Black squares show the locations of active fires
1024 detected by MODIS (Moderate Resolution Imaging Spectroradiometer) (Giglio et al., 2003).
1025 Brown dots show the location of gas flaring sites from the Global Gas Flaring Reduction
1026 Partnership (GGFR) (<http://www.worldbank.org/en/programs/gasflaringreduction>).

1027

1028 **FIGURE & TABLE CAPTIONS FOR SUPPLEMENTS**

1029

1030 **Figure S 1.** Fractional bias ($FB = [(C_m - C_o)/(C_m + C_o) \times 0.5] \times 100\%$) for all samples
1031 collected from the three campaigns in Western Siberia and northwestern European Russia in
1032 2014, 2015 and 2016. MFB (mean fractional bias) is the fractional bias averaged for all snow
1033 samples from 2014, 2015 and 2016, whereas RMSE is the root mean square error in ng g^{-1}).

1034 **Figure S 2.** (a) Distribution of snow measurements of BC adopted from Doherty et al. (2010)
1035 in the Arctic from 2005 to 2009. (b) Simulated (FLEXPART) BC concentrations in snow for
1036 the same period (right). MFB, RMSE and correlation coefficient (R) values are further given.

1037 **Figure S 3.** Timeseries of simulated and measured BC concentrations in snow collected in
1038 Alert (Macdonald et al., 2017). Correlation coefficient (R) between modelled and measured
1039 BC, RMSE and MFB values are also shown.

1040 **Figure S 4.** (a) Average footprint emission sensitivity and (b–f) source contribution (from all
1041 sources, TRA, DOM, FLR and BB) for all the samples located in northwestern European
1042 Russia.

1043 **Figure S 5.** (a) Average footprint emission sensitivity and (b–f) source contribution (from all
1044 sources, TRA, DOM, FLR and BB) for all the samples located in Western Siberia (north of 62
1045 °N).

1046 **Figure S 6.** (a) Average footprint emission sensitivity and (b–f) source contribution (from all
1047 sources, TRA, DOM, FLR and BB) for all the samples located in Western Siberia (south of
1048 62 °N).

1049

1050 **Table S 1.** Information about the samples collected in springtime of 2014, 2015 and 2016 in
1051 Western Russia.

1052

1053 **Table S 2.** $EC_{CO_2}^{corr}$ - to EC ratio (Mean \pm SD; Min - Max), showing overestimation of EC due
1054 to EC_{CO_2} - in the filtered snow samples.